# REDOX-LINKED PROTON TRANSLOCATION IN CYTOCHROME OXIDASE: THE IMPORTANCE OF GATING ELECTRON FLOW

## The Effects of Slip in a Model Transducer

DAVID F. BLAIR, JEFF GELLES, AND SUNNEY I. CHAN
*Arthur Amos Noyes Laboratory of Chemical Physics, California Institute of Technology, Pasadena, California 91125*

ABSTRACT In at least one component of the mitochondrial respiratory chain, cytochrome $c$ oxidase, exothermic electron transfer reactions are used to drive vectorial proton transport against an electrochemical hydrogen ion gradient across the mitochondrial inner membrane. The role of the gating of electrons (the regulation of the rates of electron transfer into and out of the proton transport site) in this coupling between electron transfer and proton pumping has been explored. The approach involves the solution of the steady-state rate equations pertinent to proton pump models which include, to various degrees, the uncoupled (i.e., not linked to proton pumping) electron transfer processes which are likely to occur in any real electron transfer-driven proton pump. This analysis furnishes a quantitative framework for examining the effects of variations in proton binding site $pK_a$s and metal center reduction potentials, the relationship between energy conservation efficiency and turnover rate, the conditions for maximum power output or minimum heat production, and required efficiency of the gating of electrons. Some novel conclusions emerge from the analysis, including: (*a*) An efficient electron transfer-driven proton pump need not exhibit a pH-dependent reduction potential; (*b*) Very efficient gating of electrons is required for efficient electron transfer driven proton pumping, especially when a reasonable correlation of electron transfer rate and electron transfer exoergonicity is assumed; and (*c*) A consideration of the importance and possible mechanisms of the gating of electrons suggests that efficient proton pumping by $Cu_A$ in cytochrome oxidase could, in principle, take place with structural changes confined to the immediate vicinity of the copper ion, while proton pumping by $Fe_a$ would probably require conformational coupling between the iron and more remote structures in the enzyme. The conclusions are discussed with reference to proton pumping by cytochrome $c$ oxidase, and some possible implications for oxidative phosphorylation are noted.

## INTRODUCTION

In recent years, it has become widely accepted that at least one of the components of the mitochondrial respiratory chain, cytochrome $c$ oxidase, functions as a redox-linked proton pump. In this enzyme, the flow of electrons from cytochrome $c$ at the cytosol (outer) side of the inner mitochondrial membrane to dioxygen and to protons derived from the matrix (inner) side is coupled to the electrogenic pumping of protons from the matrix to the cytosol (1). The protons so pumped contribute to the maintenance of a proton electrochemical potential (electrically negative inside) across the inner mitochondrial membrane. This proton electrochemical potential is used to drive the synthesis of ATP from ADP and inorganic phosphate which is catalyzed by another transmembranous mitochondrial enzyme, the ATP synthase (2). The

directionality of the coupled electron and proton flows in cytochrome $c$ oxidase makes the mechanism of proton translocation by this enzyme fundamentally different from the "redox loop" mechanism proposed by Mitchell (3) for the coupling sites in the respiratory chain. In the redox-loop model, electron movements across the mitochondrial membrane from the cytosol to the matrix alternate with simultaneous, electroneutral movements of electrons and protons in the opposite direction. Because of the persuasive demonstration (4) of proton pumping in cytochrome $c$ oxidase, and because of the possibility that other proton translocating elements in the respiratory chain are also electron transfer-driven proton pumps, it is important to understand the molecular mechanisms by which electron transfer reactions can be coupled to vectorial proton translocation.

This paper explores the question of how redox processes can be coupled to vectorial proton transport at a proton-pumping site consisting of a single redox center within a

---

Correspondence should be addressed to S. I. Chan.

respiratory enzyme. In particular, it investigates the role of what we will call gating of electrons (meaning the control of the rates of electron transfer into and out of the site) in such coupling. The steady-state rate equations appropriate to several models of proton pumping have been used to calculate the rate of electron transfer through the pumping site and the efficiency of free energy conversion at the site. In this way, we have begun a systematic study of the relationship between the various parameters which describe the pumping site ($pK_a$s, reduction potentials, relative electron transfer rates, etc.) and the resultant performance of the pump. The present study complements and extends earlier results that have most often been derived in terms of linear nonequilibrium thermodynamics, but it is especially concerned with particular aspects of the chemical mechanism of the pump, rather than with a phenomenological description. Our examination was originally motivated by a desire to understand published redox thermodynamic data on cytochrome oxidase as well as recent measurements of our own (5–7), and has revealed that some conclusions drawn from simple models of proton pumping (8, 9), for example, a steeply pH-dependent reduction potential of the redox center associated with pumping, are based upon implicit assumptions which are not necessarily valid in the context of a more complete treatment.

The present investigation leads to predictions regarding the likely mechanisms of proton pumping in cytochrome $c$ oxidase and clarifies which of the redox centers in this enzyme can be considered candidates for a proton-pumping site. Additionally, our analysis of a simple model transducer should complement existing treatments in the quantitative study of other biological energy transducers with which a formal analogy can be made. The analysis is particularly useful in predicting the effects of reaction slip (partial uncoupling of the driving process from the driven process) on the thermokinetic properties of the transducer. It is hoped that this predictive ability will assist in the design and interpretation of more effective experiments for clarifying the mechanisms of proton pumping in cytochrome oxidase and other enzymes.

## A SIMPLE MODEL OF REDOX-LINKED PROTON PUMPING BASED ON VARYING $pK_a$s

Many models for redox-linked proton pumping involve, with minor variations, a paradigm like that shown in Fig. 1 (8, 10). P refers to the pumping site, including whatever molecular components are necessary to the pumping action; these components include both a center that can undergo reversible oxidoreduction and a group that can reversibly bind a proton. The four states shown correspond to the four possible conditions of oxidation/reduction and protonation/deprotonation. It is assumed that a chemical mechanism exists by which the site is constrained to be protonated only from the matrix (denoted by the subscript

m) when it is reduced, and only from the cytosol (denoted by c) when it is oxidized; thus the oxidation state alone suffices to specify the accessibility of the protonating group(s). This reduces the number of states required in the description of the mechanism, and as discussed below is also in accordance with an analysis which does not implicitly give more emphasis to the regulation of proton flow than to the regulation of electron flow. The specific sequence of states drawn is not essential to the paradigm, or to the ideas we will presently develop. For example, protonation could equally well occur upon oxidation and deprotonation upon reduction (if the rules governing proton accessibility are also reversed). In the scheme in Fig. 1, each turnover cycle involves the transfer of one electron and the pumping of a single proton from the matrix to the cytosol, so in this model the $H^+/e^-$ stoichiometry is 1.

Some of the features that are important to a redox-linked $H^+$-pumping scheme like that of Fig. 1 have received particular stress in previous descriptions of such systems: first, it has been noted that an efficient pump based on such a cycle might be expected to involve some thermodynamic linkage between oxido-reduction and protolysis (a redox Bohr effect) (11, 12). This means that in the cycle drawn, reduction of the pumping site causes protonation to be favored relative to the oxidized state, i.e., $pK_a^{red}$ is greater than $pK_a^{ox}$. In this way, the affinity of the site for protons is varied cyclically during the operation of the pump. Equivalently, the pump may be considered as alternating between a state with relatively high affinity for an electron (a higher reduction potential) and a state with a lower affinity for an electron (a lower reduction poten-
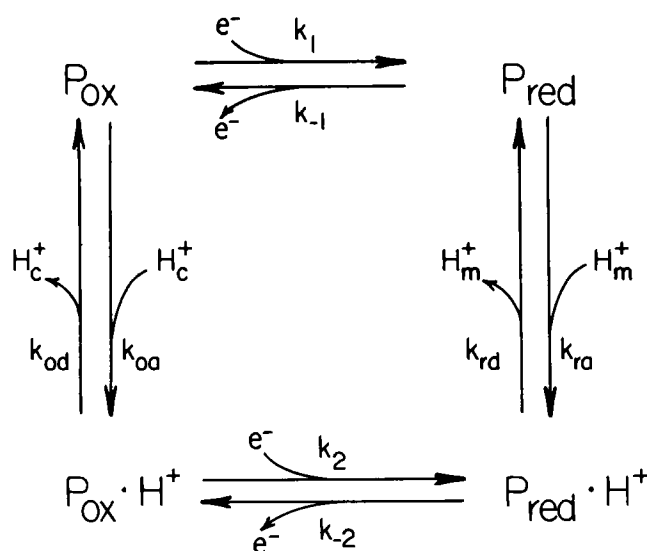


FIGURE 1 Schematic for a four-state redox-linked proton pump. Clockwise passage around the four state cycle leads to proton pumping. P refers to the pump site, including all elements (e.g. proton-conducting channels) required for pumping action; the subscripts ox and red refer to the oxidation state. Proton subscripts m and c signify the mitochondrial matrix and cytosol, respectively.

tial), depending upon whether it is protonated or not. One oxidation state of the pump is therefore matched to conditions on the electronic and protonic input sides, namely low solution redox potential and high solution pH, while the other oxidation state is matched to the conditions of high redox potential and low pH encountered on the output sides.

A feature that is essential to the operation of any real pump derived from the model in Fig. 1 is the mechanism alluded to above that controls the relative accessibilities of the site to protons derived from either the matrix or cytosol side of the membrane. In the cycle drawn, this gating of protons is necessary to prevent both protonation of the reduced state of the pump from the cytosol or deprotonation of the oxidized state to the matrix, which would lead to loss of pumping efficiency and leakage of protons across the membrane. It has been suggested (12, 13) that proton-conducting channels leading to and from a proton pumping site might play an important role in the proton pumping process, and various molecular mechanisms for proton conduction have been proposed (14, 15). The existence of specific protein-mediated transmembrane proton conduction has been demonstrated in the $F_o$ component of mitochondrial ATPase (15–19).

Proton pumping mechanisms that involve global changes of protein structure and concomitant movement of protonated protein chemical groups over relatively large distances are certainly possible in principle. However, mechanisms in which the important action is confined to the neighborhood of the pump might be expected to enable more rapid turnover. Also, the gating of electrons via some readily-envisioned mechanisms that involve nearby chemical groups (discussed below) could be very effective. In such localized proton pumping mechanisms, proton channels are essential because they facilitate the movement of the proton through most of its transmembrane passage. The rule that governs proton accessibility in the model of Fig. 1 reflects a preference for localized mechanisms: the oxidation state of the pump site (implicitly including the local geometry that it adopts in each oxidation state), rather than conformational changes involving movements of the protein at some distance from the site, solely determines the proton accessibility. The exclusion of states that differ from those shown only in their proton accessibility halves the number of states that must be specified in the cycle. Conversely, the exclusion of states that differ from those shown only in their kinetic accessibility to electrons, which also reduces the number of states that must be specified, embodies the assumption of a mechanism in which it is solely the oxidation state of the site that determines its electronic accessibility. If no assumptions are made, the number of states formally required is actually 16 (not eight, as has sometimes been implied [12]). Since it suffices for demonstration of the ideas presently under consideration, we have pursued the simplest analysis possible, in which redox state solely determines both proton and electron accessibilities. The detailed conclusions of our analysis would not be changed by a more explicit consideration of more conformational states, if, as discussed below, proton motions are rapid relative to electron transfers.

The requirement for control of electron flow in a proton pumping scheme like that in Fig. 1 has been noted previously (20–23), but its implications for the mechanisms of redox-linked proton pumping have not been explored. The theory of electron transfer rates is quite well developed and makes predictions that are often readily testable. It therefore represents a valuable resource for the bioenergeticist seeking to understand redox-linked proton pumping.

The emphasis that has been given to thermodynamic linkage of oxidoreduction to protolysis and to the regulation of proton flow has led the authors of some proton pump models to assume implicitly that these two factors exert primary control over the proton pumping cycle (8, 9, 12). In this kind of proton pump model, which could be called a "$pK_a$-controlled" pump, thermodynamic linkage together with the gating of protons cause the site to alternate between a state that has a high proton affinity and is accessible only to protons from the matrix, and a state that has a low proton affinity and is accessible only from the cytosol. Alternation between two states so defined would necessarily lead to proton pumping. However, the mechanism of alternation between these states, which involves electron transfer to and from the pumping site, is obscured by this perspective. The rates of these electron transfers will in general depend upon whether the site is protonated or not, because electron transfer rates are dependent upon the structures and reduction potentials of the electron transfer partners (22, 24, 25). Hence it is important to consider the probable nature of these effects and their consequences for the design of an efficient proton pump.

$pK_a$-controlled mechanisms of proton pumping merit particular discussion because they make a clear prediction regarding the reduction potential of the proton pumping site. Since reduction leads to substantial protonation ($pK_a^{red}$ is higher than the pertinent solution pH) and oxidation causes substantial deprotonation ($pK_a^{ox}$ is lower than the pertinent solution pH), the pumping site should exhibit a reduction potential that is steeply (approximately −60 mV/pH unit) dependent upon pH in the physiological range (26) (Fig. 2). A site that has a pH-dependent reduction potential would thus appear more likely to pump protons than one that does not. This reasoning has sometimes been used to implicate one site ($Fe_a$) in the proton pumping function of cytochrome $c$ oxidase and to disqualify another ($Cu_A$) (8, 12). However, recent spectroelectrochemical measurements suggest that neither of these sites displays this type of strongly pH-dependent potential. This issue will be reconsidered following the development of our analysis of redox-linked proton pumping.

## THE REGULATION OF ELECTRON FLOW
## IN REDOX-LINKED PROTON PUMPS

Paradigms like that depicted in Fig. 1 are symmetrical with respect to electron and proton movements, meaning that electrons and protons play analogous roles during the pumping cycle when they are viewed simply as ligands to the pumping site. There is therefore no reason to emphasize gating of protons more than gating of electrons. In fact, efficient gating of electrons may be more difficult to achieve because of the delocalized character of electrons and their associated capacity for tunneling. The redox loop mechanism of Mitchell, which adequately describes some of the other coupling sites in the respiratory chain, is appealing in part because the steps involving the passage of net charge through the membrane need only involve electrons, which will be less hindered by the electrically insulating barrier posed by the mitochondrial membrane than charge-bearing atoms or molecules which are not able to tunnel over appreciable distances.

The nature of mechanisms for gating electron flow and the consequences of ineffective regulation of electron flow may be fruitfully explored within the framework of electron transfer rate theory. To this end, it is helpful to outline briefly some of the central concepts of this theory as elaborated, for example, by Marcus (24, 27) or Hopfield (21, 22). It should be emphasized that this field is currently very active and that many of the ideas are just beginning to

be tested systematically in protein model systems (28–30), which are the most relevant to the present discussion.

At least four factors are important in determining the rate of an electron transfer reaction. The first of these is the reaction exergonicity. Under all but extraordinary conditions, a more exergonic electron transfer reaction is expected to proceed more rapidly than a less exergonic (but otherwise identical) reaction (22, 27). This factor will always operate against energy conservation, since uncoupled processes (i.e., those in which electron transfer through the pump is not accompanied by proton pumping) are more exergonic than coupled ones. In many cases, probably including the present one, a change in the reaction free energy will be manifested as a change in the activation energy for the reaction which is about one-half as large (22, 27, 31). We will take advantage of this useful approximation in our kinetic treatment of proton pump models. Similar assumptions have previously been made in modeling the voltage dependence of transmembrane charge-translocating reaction steps, by Laüger (32), Hansen et al. (33), and recently by Pietrobon and Caplan (34). The validity of such approximations must of course be tested experimentally whenever possible, but it is noteworthy that in the case of electron transfer, owing largely to the simplicity of this fundamental chemical reaction, this approximation is likely to be reasonably accurate.

A second factor that influences electron transfer rates is the so-called reorganizational energy associated with the electron transfer. This refers to the amount of energy involved in the structural rearrangements that accompany the oxidation of the electron donor and the reduction of the electron acceptor. For reactions that are not extremely exergonic, including those of mitochondrial electron transport, a smaller rearrangement energy will lead to more rapid electron transfer. Since the rearrangement energy involves the details of the coordination geometry of the electron transfer partners, it should be possible to modulate it significantly by changing the coordination environment, for example by protonating a ligand or exchanging one ligand for another, at the pumping site. However, modulation of electron transfer rates via this mechanism is expected to be approximately scalar in character, meaning that the rates of electron transfer to and from the pump will be changed by similar factors. This kind of regulatory mechanism cannot by itself give rise to the desired vectorial process of proton translocation.

A third factor influencing electron transfer rate is the distance between the electron donor and acceptor. Electron transfer over long distances in proteins involves thermally activated tunnelling whose probability is related to the extent of overlap between the tails of the donor and acceptor orbitals. The amplitudes of these tails will decrease rapidly with distance in a protein and in the reduction potential range relevant to mitochondrial electron transfer. If other factors remain fixed, it is expected that the electron transfer rate could decrease by a factor as
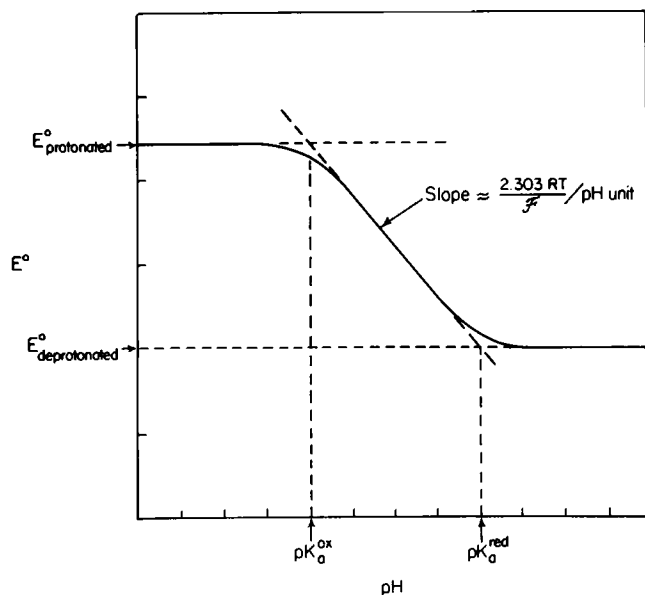


FIGURE 2   The dependence of reduction potential upon pH for a redox couple in which reduction is strongly linked to protonation. In the pH range between $pK_a^{red}$ and $pK_a^{ox}$, the reduction potential exhibits a steep pH dependence (~60 mV/pH unit for a one-electron, one-proton acceptor at 303 K). This would be the behavior anticipated for a proton pump in which $pK_a$ changes were of greatest importance in defining the most probable reaction path, which requires $pK_a^{ox}$ to be considerably less than 7 and $pK_a^{red}$ to be considerably greater than 7.

large as 100 for every 3-Å increase in distance (22, 35, 36). Conformational changes which change the intersite distances by even a few Ångstroms will therefore have a significant effect. If a continuous range of different protein conformations is thermally accessible, it is likely that in some of these conformations the electron transfer rate will be especially fast, owing to the effects of the intersite distance and the intersite material (described below). In such a case, a handful of the many accessible conformational states could make the dominant contributions to the electron transfer rate.

A final factor, which is also related to the overlap of donor and acceptor orbitals, is the nature of the intersite material. The donor and acceptor orbital amplitudes will decrease with distance more rapidly in a saturated hydrocarbon environment or in a vacuum than in regions containing aromatic groups or other conjugated systems, if the symmetry of the aromatic orbitals permits interaction with the donor and acceptor orbitals. Particular alignments of hemes, coordinated or noncoordinated histidyl imidazoles, or other aromatic amino acid side chains could therefore enhance the rate of electron transfer. The possible magnitude of such an effect is a matter currently under study (37, 38), but it is likely to be quite large. Fairly minor structural changes could have a significant impact on electron transfer rates, since symmetry restrictions could cause some orbital overlaps to vanish at particular orientations of aromatic amino acid side chains. Since the thermally activated electron tunnelling is not restricted to a single well-defined pathway connecting the redox sites, structural changes close to the sites could more effectively modulate the tunnelling probability than changes farther away.

The role of gated electron flow in redox-linked proton pumping is depicted in Fig. 3. The reaction cycle drawn is an elaborated version of the four-state scheme in Fig. 1; the electron donor and acceptor are explicitly identified and the electron transfer reactions that can uncouple electron transport from proton pumping (the "electron leaks") are shown. The electron leaks shown are expected to be significantly exergonic, so the reverse processes, which would be much slower, have been ignored. A rate constant is assigned to each of the various electron and proton transfer processes. Vectorial regulation of proton flow is recognized as before by the proton subscripts m and c, and this regulation is assumed to be perfect. Uncoupling processes involving protonation/deprotonation (the vertical segments of the cycle in Fig. 3) are therefore ignored. The generalization to imperfect gating of protons is not difficult but would obscure the central points of the present analysis, which emphasizes regulated electron flow. We note that even with perfect gating of protons, the pumping site may nevertheless exhibit less than perfect pumping efficiency, and even net proton flux in the "wrong" direction, because of the presence of the electron leaks. (A negative proton flux would result if the reaction followed the
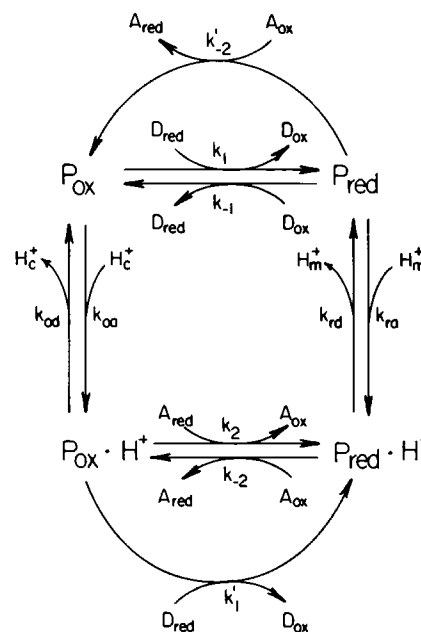


FIGURE 3   Four-state redox-linked proton pumping cycle that includes electron leak pathways. The electron donor and acceptor are signified by D and A, respectively. The uncoupled electron transfers are assigned primed rate constants; the reverse of the uncoupled processes are not included since they are expected to be much slower.

outermost pathway in Fig. 3, involving both uncoupled electron transfers, in the counterclockwise direction.)

The importance of effective electron gates is readily appreciated if one considers the free energy changes associated with the reactions diagrammed in Fig. 3. As noted above, $pK_a$-controlled proton pumps are based upon a thermodynamic linkage between oxido-reduction and protolysis. The $pK_a$ of the reduced pump will therefore be different from (in a scheme like Fig. 3, greater than) the $pK_a$ of the oxidized pump, and the reduction potential of the site will be greater when it is protonated than when it is not. Hence the uncoupled process $k'_1$ in Fig. 3 will be more exergonic than the coupled process $k_1$, by an amount equal to the thermodynamic linkage. The same is true of the uncoupled process $k'_2$ relative to the coupled process $k_2$. Without special provisions for directing the electron transfers, the rate constants for the more exergonic, uncoupled processes will be greater, and efficient proton pumping will not occur. Adopting the relation between electron transfer rate and exergonicity described above, it can be shown that in the limiting case of a proton pump that relies exclusively on thermodynamic linkage (so that the uncoupled and coupled isoergonic electron transfer rates are equal) net pumping of protons against an opposing gradient is not possible (see discussion of Fig. 5 below).

Having recognized the importance of gating of both protons and electrons, we may envisage proton pumps that might be called "kinetically controlled" pumps. In their most extreme form, kinetically controlled pumps would involve no thermodynamic linkage (no modulation of $pK_a$s)

but would rely exclusively upon the gating of electrons and protons. In a less extreme form, kinetic control would play a significant role in the pumping cycle, and thermodynamic linkage would assume a correspondingly diminished role. As the foregoing discussion indicates, a degree of kinetic control is essential. Electron leakage is an issue that should be considered in any type of model for a redox-linked proton pump, because it can place significant constraints on the overall efficiency of a real pump, and because any real pump must incorporate mechanisms for minimizing it.

## KINETIC ANALYSIS OF A PROTON PUMPING MODEL THAT INCLUDES UNCOUPLED PATHWAYS

### Solution of the Steady-State Rate Equations

In this section, we will undertake a quantitative investigation of the importance of gating electron movements, the role of thermodynamic linkage, and related issues involved in redox-linked proton pumping. The approach is based upon the solution of the steady-state rate equations which describe various pumps, and is in some respects similar to the work of Laüger (39), who considered the case of perfect gating, and to the more recent study of Pietrobon and Caplan, who examined some of the effects of leaks on steady state flow-force relationships and made a critical comparison of their results with the equations of linear irreversible thermodynamics (34). The analysis is based upon the four-state reaction scheme given in Fig. 3. The important assumptions implicit in this reaction scheme have been noted above.

The present analysis addresses the steady state rather than the equilibrium condition of a proton pump, and thus reveals kinetic properties. Any real proton pump must operate at a nonzero rate to be useful, which will entail some irreversibility in the reaction cycle and an accompanying departure from maximum efficiency. It is interesting to inquire at what level of efficiency (and hence rate) a real proton pump is likely to operate, and how this level of operating efficiency is related to the magnitudes of the electron or proton leaks that are present. The answer to this question must involve the relationship of the efficiency of the pump to its turnover rate, and the relationship of both to the electron or proton leaks. These relationships are readily predicted using a steady-state analysis. A steady-state analysis is probably applicable to mitochondria that are in a particular sustained state of respiration. However, it is not directly applicable to the transient behavior which has so far been observed in measurements of proton pumping stoichiometry in cytochrome $c$ oxidase (40, 41). These experiments typically involve measurement of the initial rate of pH changes following a pulse of reductant or oxygen; the membrane potential is initially zero and rapidly increases as protons are pumped, ordinarily not reach-

ing physiological values. Conversely, it should be noted that transient measurements of proton pumping stoichiometry should not be extrapolated uncritically to the mitochondrial steady state.

Previous treatments (references 42–46, for example) of the kinetics of mitochondrial energy transduction have most often been more phenomenological, using the formalism of irreversible thermodynamics under the assumptions of linear flow-force relationships and Onsager reciprocity. To a surprising degree, the flow-force relationships measured in mitochondrial oxidative phosphorylation are in accord with these assumptions (43, 45). The recent investigation by Pietrobon and Caplan (34) most nearly resembles our own. These authors solved steady-state rate equations in order to calculate force-flow relationships for two different proton pumps that incorporated various degrees of uncoupling via a single slip pathway. Their approach, like that described here, is complementary to the irreversible thermodynamic approach in that it begins with a particular molecular model for transduction and makes predictions that can be compared with those of irreversible thermodynamics. By critically evaluating the assumptions of the irreversible thermodynamic treatment in the light of their steady-state analysis, Pietrobon and Caplan determined that the nonequilibrium thermodynamic approach is an approximation to be used with some caution. The particular advantage of the steady-state approach is that reaction slip and other pertinent phenomena are given more precise physical meaning in terms of rate constants for particular reaction steps in a chemical mechanism.

A depiction of the four-state pumping cycle that emphasizes the irreversibility of the reaction is given in Fig. 4. In this figure, the electron and proton standard free energy changes at each reaction step are given in terms of the various reduction potentials and $pK_a$s that describe the pump. The figure is intended to introduce some of the symbols (reduction potentials and $pK_a$s) which are important in later discussion and facilitates the visualization of the corresponding quantities.

The free energies shown in Fig. 4 reflect the energetic scheme most commonly assumed for a "$pK_a$-controlled" proton pump; i.e., protonation from the matrix is somewhat exergonic in the reduced state and deprotonation to the cytosol is somewhat exergonic in the oxidized state. Also, the reduction of the deprotonated pump by the donor and the oxidation of the protonated pump by the acceptor are both slightly exergonic. This is in accordance with the presumed requirement, noted above, for matching of the input and output states of the pump to input and output potentials. While the figure is drawn to reflect particularly this conventional type of pump, the analysis that follows will extend to a range of pump "designs," some of which will have state energies that do not resemble those in Fig. 4. For example, if the $pK_a$ of the reduced pump site were decreased, the second reaction step in Fig. 4 would be correspondingly less exergonic.
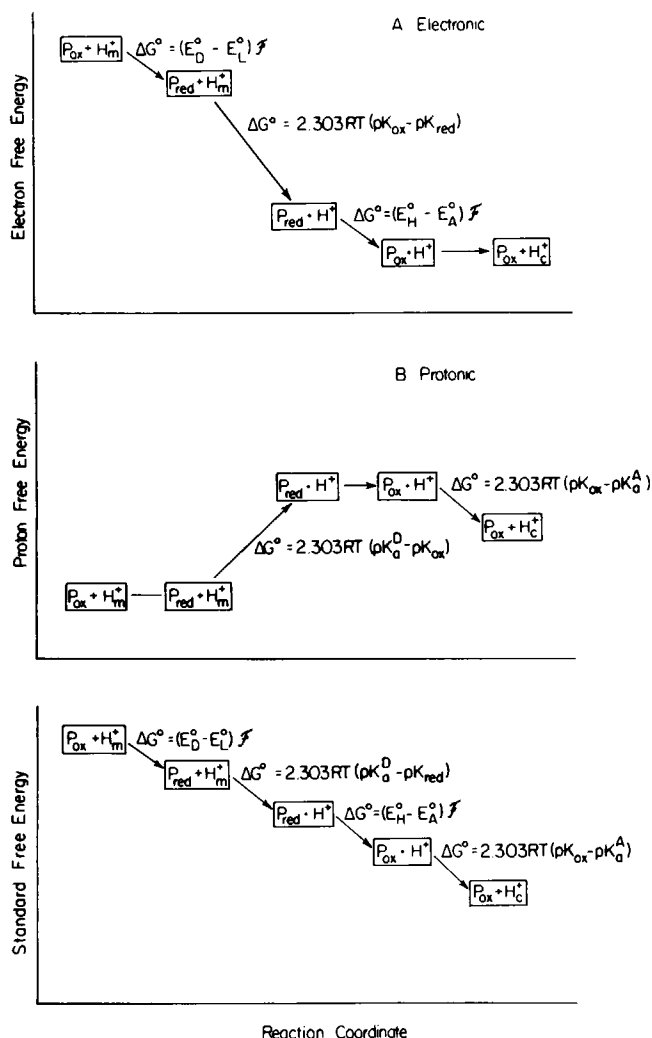
A  Electronic

$P_{ox} \cdot H_m^+$  $\Delta G^{\circ} = (E_D^{\circ} - E_L^{\circ}) \mathcal{F}$

$P_{red} \cdot H_m^+$

$\Delta G^{\circ} = 2.303 RT (pK_{ox} - pK_{red})$

$P_{red} \cdot H^+$  $\Delta G^{\circ} = (E_H^{\circ} - E_A^{\circ}) \mathcal{F}$

$P_{ox} \cdot H^+$  ⟶  $P_{ox} + H_c^+$

B  Protonic

$P_{red} \cdot H^+$ ⟶ $P_{ox} \cdot H^+$  $\Delta G^{\circ} = 2.303 RT (pK_{ox} - pK_a^A)$

$P_{ox} + H_c^+$

$\Delta G^{\circ} = 2.303 RT (pK_a^D - pK_{ox})$

$P_{ox} + H_m^+$ ⟶ $P_{red} \cdot H_m^+$

$P_{ox} + H_m^+$  $\Delta G^{\circ} = (E_D^{\circ} - E_L^{\circ}) \mathcal{F}$

$P_{red} + H_m^+$  $\Delta G^{\circ} = 2.303 RT (pK_a^D - pK_{red})$

$P_{red} \cdot H^+$  $\Delta G^{\circ} = (E_H^{\circ} - E_A^{\circ}) \mathcal{F}$

$P_{ox} \cdot H^+$  $\Delta G^{\circ} = 2.303 RT (pK_{ox} - pK_a^A)$

$P_{ox} + H_c^+$

Reaction  Coordinate

FIGURE 4  Standard free energy changes that occur in the four-state
proton-pumping cycle of Fig. 3. The expressions for free energy changes
for the electron transfer reactions assume that the donor and acceptor are
50% reduced, so that the operating potentials equal the standard poten-
tials. The standard free energy changes are partitioned formally into the
electronic ($A$) and protonic components ($B$); see the text for a description
of this convention and its limitations. The symbols used are: $E_D^{\circ}$, the
standard reduction potential of the electron donor to the pump; $E_A^{\circ}$, the
standard reduction potential of the electron acceptor; $E_L^{\circ}$, the standard
reduction potential of the deprotonated state of the pump; $E_H^{\circ}$, the
standard reduction potential of the protonated state of the pump; $pK_a^{red}$,
the $pK_a$ of the reduced pump; $pK_a^{ox}$, the $pK_a$ of the oxidized pump. For the
purpose of illustrating the standard free energy changes accompanying
proton transfers to and from the aqueous phases, we have represented the
solvent by protonatable donor and acceptor groups with $pK_a$s, $pK_a^D$, and
$pK_a^A$ equal to the matrix and cytosol pH, respectively. Actual (as opposed
to standard) free energy changes of proton transfer to the bulk solvent
were incorporated in the calculations described in the text.

Hill (47) has pointed out that there is no unique way to
partition the free energy changes at each reaction step in a
transduction cycle like that in Fig. 3 into individual
components due to each of the two ligands (in this case, the
proton and the electron), because the free energy of an
enzyme-ligand complex cannot be assigned to the ligand

alone, and because the free energy of a complex containing
two ligands cannot be partitioned between the two ligands.
It therefore cannot be stated that the electron "transfers"
its free energy to the proton to be pumped in one particular
reaction step. For purposes of illustration, however, we
have in Fig. 4 adopted a convention that formally partitions
the free energy changes between the proton and the
electron. The particular convention employed is that the
increase in reduction potential that takes place when the
site is protonated is associated with a corresponding stabili-
zation of the electron. The other free-energy changes in
Fig. 4 follow accordingly. The free energy scheme shown is
intended to illustrate that by appropriate selection of the
$pK_a$s and reduction potentials, it is possible for the transfer
of free energy from electrons to protons to take place
without requiring very large changes in the standard free
energy of the system as a whole at any step, in spite of the
large protonic and electronic net free energy changes that
must take place over the whole cycle.

In Fig. 4, the initial state $P_{ox} + H_m^+$ and the final state
$P_{ox} + H_c^+$ differ in protonic free energy by the magnitude
of the proton electrochemical potential across the mem-
brane. In an energized mitochondrion, this potential corre-
sponds to a protonmotive force (see reference 3) of ~200
mV (48–53). With respect to electronic free energy, the
initial and final states will differ by the difference between
the reduction potentials of the electron donor and acceptor.
(Note that the free energies given in Fig. 4 are free
energies under standard conditions, corresponding to donor
and acceptor both one-half reduced.) In the case of cyto-
chrome $c$ oxidase, for example, the standard reduction
potential difference will be approximately 550 mV (for the
average of the four different electron transfers required to
reduce dioxygen to water), and approximately half of the
free energy change from transferring an electron across
this potential difference will be available for proton pump-
ing, since the electron transfers to dioxygen are themselves
electrogenic (4).

The rate of proton pumping in the reaction scheme of
Fig. 3 is given by

$$R_{H^+} = k_{ra}[H_m^+][P_{red}] - k_{rd}[P_{red} \cdot H^+]. \tag{1}$$

The rate of electron transfer is given by

$$R_{e^-} = k_1[D_{red}][P_{ox}] + k_1'[D_{red}][P_{ox} \cdot H^+]$$
$$- k_{-1}[D_{ox}][P_{red}]. \tag{2}$$

Defining the flow ratio of proton pumping by

$$X = R_{H^+}/R_{e^-}, \tag{3}$$

the overall efficiency of the pump is then

$$\eta = X(\Delta\tilde{\mu}_{H^+}/\Delta G), \tag{4}$$

where $\Delta\tilde{\mu}_{H^+}$ is the proton electrochemical potential across
the membrane, and $\Delta G$ is the total free energy per electron

transfer available for proton pumping (equal to the free energy available from electron transfer in the absence of a membrane electrical potential less the free energy required for charge translocation across the existing membrane potential). The other symbols are defined by reference to Fig. 3.

The equations that describe the steady-state condition of a pump like that in Fig. 3 can be solved by standard methods, as shown in the Appendix. The resulting expressions for the steady-state concentration of each of the four species were used in Eqs. 1 and 2 to derive the following expressions for the rate of electron transfer through the pump and the flow ratio of proton pumping

$$R_{e^-} = A/B \qquad (4)$$

$$X = C/A. \qquad (5)$$

Where

$$A = k_1 [D_r] \{k_{rd}k'_{-2}[A_o](k_{od} + k_2 [A_r] + k'_1 [D_r])$$

$$+ k_{od}k_{-2}[A_o](k'_{-2}[A_o] + k_{ra}[H_m^+])\}$$

$$+ k'_1 [D_r] \{k_{rd}k_{oa}[H_c^+] k'_{-2} [A_o]$$

$$+ k_{ra}[H_m^+] k_1 [D_r] k_{-2}[A_o]$$

$$+ k_{oa}[H_c^+] k_{-2}[A_o](k'_{-2}[A_o] + k_{-1}[D_o]$$

$$+ k_{ra}[H_m^+])\}$$

$$- k_{-1}[D_o]k_2[A_r] k_{oa}[H_c^+] k_{rd},$$

$$B = \{k_{-2}[A_o] (k_{od} + k_{oa}[H_c^+]) + k_{oa}[H_c^+] (k_2[A_r]$$

$$+ k'_1[D_r])\} \{k'_{-2}[A_o] + k_{-1}[D_o] + k_{ra}[H_m^+]\}$$

$$+ \{k_{rd}(k'_{-2}[A_o] + k_{-1}[D_o] + k_1[D_r])$$

$$+ k_{ra}[H_m^+] k_1[D_r]\} \{k_{od} + k_2[A_r] + k'_1[D_r]\}$$

$$+ k_{oa}[H_c^+] k_{rd} (k_2[A_r] + k'_1[D_r] + k'_{-2}[A_o] + k_{-1}[D_o]$$

$$+ k_1[D_r] k_{-2}[A_o] (k_{ra}[H_m^+] + k_{od}),$$

$$C = k_{ra}[H_m^+] k_{-2}[A_o]k_1[D_r]k_{od} - k_{oa}[H_c^+]k_{rd} (k'_{-2} [A_o]$$

$$+ k_{-1}[D_o]) (k_2[A_r] + k_1'[L_r])$$

and the various symbols are defined in Table I and Fig. 3. These expressions were employed to calculate electron transfer rates and proton pumping efficiencies, using various values for the kinetic parameters that describe the pump. Description of the input parameters and the values assigned to them in the initial analysis are given in Table I; the available free energy for proton pumping and input/output potentials are intended to approximate cytochrome oxidase. Rates and efficiencies were calculated for transmembrane proton electrochemical potentials ranging from zero to a potential equal to the total free energy available to the pump. This transmembrane proton electrochemical potential is the maximum attainable at steady state and can only occur in the case of perfect pumping efficiency.

The following assumptions were made regarding the

TABLE I.
PARAMETERS USED IN THE CALCULATION OF RATES AND EFFICIENCIES OF THE FOUR STATE REDOX LINKED PROTON PUMP

| Parameter | Description | Value used in initial analysis |
|---|---|---|
| $E_D^o$ | Reduction potential of the electron donor to the pump | 250 mV |
| $E_A^o$ | Reduction potential of the electron acceptor from the pump | 550 mV |
| $[D_r]$ | Concentration of the reduced form of the donor relative to that of the pump | 0.5 |
| $[D_o]$ | Concentration of the oxidized form of the donor relative to that of the pump | 0.5 |
| $[A_r]$ | Concentration of the reduced form of the acceptor relative to that of the pump | 0.5 |
| $[A_o]$ | Concentration of the oxidized form of the acceptor relative to that of the pump | 0.5 |
| $E_L^o$ | Reduction potential of the deprotonated pumping site (Fig. 3, upper redox equilibrium) | 310 mV |
| $E_H^o$ | Reduction potential of the protonated pumping site (Fig. 3, lower redox equilibrium) | 490 mV |
| $pK_a^{red}$ | $pK_a$ of the reduced pump site | 10.0 |
| $pK_a^{ox}$ | $pK_a$ of the oxidized pump site | 7.0 |
| $PP_i$ | Product of the rates of protonation and deprotonation on the input (matrix) side of the pump. This quantity is related to the height of the barrier to protonation/deprotonation, and thus describes the kinetics of proton movements. | $1 \times 10^{15}$ s$^{-2}$ |
| $PP_o$ | Product of the rates of protonation and deprotonation on the output (cytosol) side of the pump | $1 \times 10^{15}$ s$^{-2}$ |
| $EP_i$ | Product of the forward and backward rates of electron transfer on the input side of the pump. The electron transfer analog of $PP_i$. | $1 \times 10^4$ s$^{-2}$ |
| $EP_o$ | Product of the forward and backward rates of electron transfer on the output side of the pump | $1 \times 10^4$ s$^{-2}$ |
| $KL_i$ | Standardized* rate of the electron leak involving the electron donor | |
| $KL_o$ | Standardized* rate of the electron leak involving the electron acceptor | |

*By "standardized," it is meant that these rate constants apply for the electron transfers in question when the processes are isoergonic. To obtain actual rate constants, the standard rates were adjusted under the assumption that changes in $\Delta G$ are manifested as changes in $\Delta G\ddagger$, which are one-half as large, consistent with the discussion (see text) of the factors that influence electron transfer rates. In this way, the anticipated effect of changes in $E_L^o$ or $E_H^o$ upon the rates of electron leakage are automatically taken into account. Note that the standard rates for the coupled electron inputs and outputs are simply the square roots of $EP_i$ and $EP_o$.

mitochondrial electrochemical proton gradient. First, the pH in the cytosol was assumed not to vary, since it ordinarily involves a buffering capacity that is large relative to the interior of the mitochondrion. The cytosol pH was fixed at 7.0, which is a reasonable estimate of intracellular pH. For the initial analysis, the electrochemical proton potential was treated as consisting only of a pH difference, with no electrostatic component. Calculations that explicitly included an electrostatic component (not shown) demonstrated that this simplification does not change the principal conclusions to be drawn from the analysis, and required knowledge of quantities that can only be guessed at present (specifically, the locations of the pump site, the electron donor, and the electron acceptor within the transmembrane profile of electrostatic potential). The effects of an electrical membrane potential are readily determined, especially if it is assumed that channels conduct protons to and from the site: The electron transfer exergonicities, and hence rates, will change in accordance with the electrical potential difference between the participating sites. The effective proton activities at the pump will be changed by an amount that reflects the work required to transport protons to and from the site under the influence of the transmembrane electric field (64). The latter effect is important in determining the effective values of pH sensed by the pump, and will influence its optimal $pK_a$ values accordingly.

To emphasize the fact that it is the pH values of the compartments that are being varied, transmembrane proton electrochemical potentials are expressed as the corresponding $\Delta pH$ in the analysis that follows. The proton electrochemical potential difference associated with a pH gradient ($\Delta pH$) is given by the equation $\Delta \bar{\mu}_{H^+} = 2.303 (RT/\mathcal{F}) \Delta pH$. For simplicity, a temperature of 30° was assumed so that 1 pH unit corresponds to 60 mV. A transmembrane proton chemical potential difference of 3 pH units would correspond to an effective matrix pH of 10.0. (We do not suppose that the pH of the mitochondrial matrix is actually this high; this value is an effective pH that reflects both the proton activity in the matrix and the effects of the transmembrane electric field upon proton activities at the pump. If the pump were situated at the cytosol end of a proton channel traversing the membrane, the pH it experiences when exposed to the matrix would be roughly this high, given a typical transmembrane proton electrochemical potential of 200 mV.)

## Pump Rates and Efficiencies: Effects of Transmembrane ΔpH and Electron Leaks

Both the rate of electron transfer through a proton pumping site and the efficiency of the proton pumping are expected to depend upon the magnitude of the transmembrane proton electrochemical gradient. In Fig. 5, the predicted efficiency of the proton pump (calculated according to Eqs. 4 and 5) is plotted as a function of the
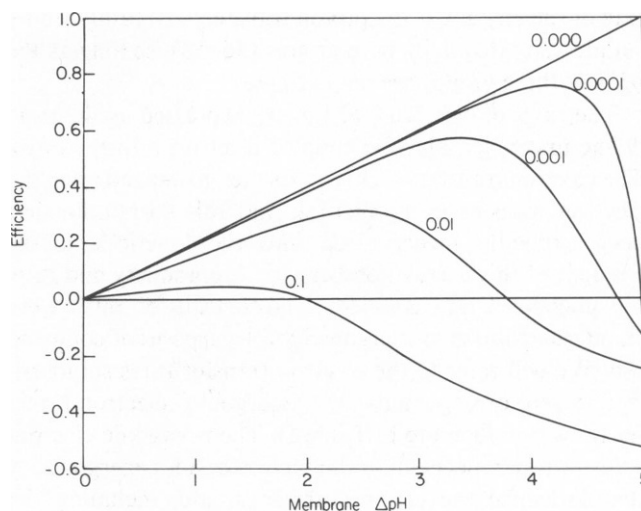


FIGURE 5 Efficiency of the proton pump model (Fig. 3) as a function of the mitochondrial membrane pH gradient, for five different values of the rates of uncoupled electron transfer (electron "leak rates"). The electron leak rate is expressed in the figure as the ratio of the isoergonic uncoupled and coupled electron transfer rates (for the motivation behind this comparison of isoergonic electron transfer rates, see the text and the footnote to Table I). The values of the parameters that describe the pump (see Table I) are as follows: $E_D^o = 250$ mV; $E_A^o = 550$ mV; $E_L^o = 310$ mV; $E_H^o = 490$ mV; $[D_r] = [D_o] = [A_r] = [A_o] = 0.5$; $pK_a^{red} = 10.0$ ($pK_a^{ox}$ thus equals 7.0); $PP_i = PP_o = 1 \times 10^{15}$ s$^{-2}$; $EP_i = EP_o = 1 \times 10^4$ s$^{-2}$. Since $EP_i$ and $EP_o$ are 1 × 10$^4$ s$^{-2}$, the isoergonic coupled electron transfer rate is 100 s$^{-1}$, or the square root of 1 × 10$^4$. Note that these parameters are symmetric with respect to the input and output sides of the pump; i.e., $PP_i = PP_o$, $EP_i = EP_o$, $E_L^o - E_D^o = E_A^o - E_H^o$, etc.

magnitude of the membrane ΔpH for four different values of the electron leak rates. The other parameters were selected to preserve symmetry (with respect to the relationship of the pump $pK_a$s to the pH gradient across the membrane, and the relationship of the pump reduction potentials to the donor and acceptor reduction potentials), and to attain a near-optimum in kinetic performance. In all cases examined below, the rate of protonation has been assumed to be fast relative to the electron transfer rates. This is in accordance with the present emphasis on electron transfer and the gating of electrons. The assumption that protonation is fast relative to electron transfer is also in accordance with what is known about the intersite distances in cytochrome c oxidase. The $Fe_a$ and $Cu_A$ sites are a considerable distance, probably 15 Å or more, away from each other and from the $Fe_{a_3}/Cu_B$ site (54). Electron transfer over such a distance is not expected to take place much faster than the overall turnover rate that the enzyme can achieve under uncoupled conditions [~100 s$^{-1}$ (55)], unless the reorganizational energy and electron transfer exergonicity are optimally related in a way that appears unlikely given the small exergonicities under consideration (22). Hence, rapid preequilibria involving electron transfer between the pump site and the other sites in the enzyme appear unlikely. On the other hand, protonation/deprotonation could be considerably faster than the overall turnover

rate of the enzyme if the proton transfers are catalyzed by suitably situated acid/base groups (56–58), so long as the $pK_a$s of these groups are not extreme.

The rates of electron leakage are expressed as the ratio of the uncoupled and the coupled electron transfer rates. The electron transfer rates are expected to depend upon the electron transfer exergonicities, and this correlation has been explicitly incorporated into the kinetic analysis. Because of this correlation between exergonicity and rate, the uncoupled and coupled electron transfer rates were standardized to zero exergonicity for purposes of comparison. We will refer to the electron transfer rates standardized to zero exerogonicity the "isoergonic" electron transfer rates (see footnote to Table I). The isoergonic electron transfer rate reflects all of the factors besides exergonocity that influence the electron transfer rate, including the intersite distance, the nature of the intervening material, and the reorganizational energies. It is these factors that can be manipulated to achieve gating of electrons, so the uncoupled/coupled isoergonic electron transfer rate ratio measures the effectiveness of gating.

It is evident from Fig. 5 that the rate of uncoupled electron flow has a dramatic effect on the efficiency of the pump. When the ratio of the uncoupled and coupled isoergonic electron transfer rates is zero (perfect control of electron flow), the efficiency attains a value of 1.0 when the membrane proton electrochemical potential equals the available free energy (this occurs at $\Delta pH = 5$ for the parameters used in Fig. 5). When the uncoupled/coupled ratio is 0.0001, the maximum attainable efficiency is 0.76, and when this ratio is increased to 0.001, the maximum efficiency decreases to 0.57. At a ratio of 0.01, which still involves significant gating of electron flow, the maximum efficiency is only 0.31. At a ratio of 1.0, corresponding to no gating of electron flow, the efficiency is zero at zero membrane potential and negative (i.e., cycling causes discharge of the membrane potential) for all nonzero membrane potentials (data not plotted). This last result is of course not a coincidence, but follows in consequence of the particular correlation between electron transfer rate and exergonicity that we have assumed, which causes the effects of the thermodynamic factor ($pK_a^{ox} - pK_a^{red}$) to be exactly compensated by kinetic factors. Assuming a weaker correlation would lead to quantitatively different predictions, but the basic conclusion (i.e., that control of electron flow is very important) would hold until the correlation was made surprisingly weak.

Fig. 5 indicates that in the presence of electron leaks there is a membrane potential that is optimal for the efficiency of the pump. However, in most cases simulated, the efficiency does not decrease very sharply away from this optimum, so that relatively efficient operation is possible over a substantial ($\pm \sim 20\%$) range of membrane $\Delta pH$. The curves in Fig. 5 are very similar to the analogous curves generated by analyses based upon linear nonequilibrium thermodynamics by, for example, Caplan (51),

Stucki (43), or Rottenberg (42). The curve describing an uncoupled/coupled isoergonic rate ratio of 0.0001 corresponds approximately to a phenomenological degree of coupling $q$ of ~0.99, and that describing a rate ratio of 0.01 to a degree of coupling of ~0.8 (43).

In respiring mitochondria and in vesicle-reconstituted cytochrome $c$ oxidase, the rate of electron transfer decreases as the transmembrane proton electrochemical potential increases (50–53, 60, 61). This phenomenon is a manifestation of "respiratory control," and the ratio of the electron transfer rate in phosphorylating (State 3) mitochondria (in which the proton gradient is partially discharged by the ATP synthase) to the rate in fully membrane-energized (State 4) mitochondria is called the "respiratory control ratio" (62). This kind of behavior, reflecting control of the electron transfer rate by the thermodynamic force opposing proton pumping, is illustrated in Fig. 6, which plots the rate of electron transfer through the pump as a function of the membrane $\Delta pH$ (for the same parameters used in Fig. 5). The electron transfer rate decreases sigmoidally with increasing membrane $\Delta pH$, and in the case of perfect gating (no electron leakage) the rate becomes zero when the applied potential equals the available free energy (5.0 pH units), as required at equilibrium. As gating is made less effective, the decrease in rate with increasing membrane $\Delta pH$ becomes less severe. When the uncoupled/coupled rate constant ratio is 0.01, the electron transfer rate is still at ~50% of its maximum value when $\Delta pH = 5$. With uncoupled/coupled ratios 10-fold or larger, an increase in electron transfer rate with increasing membrane potential is predicted (calcula-
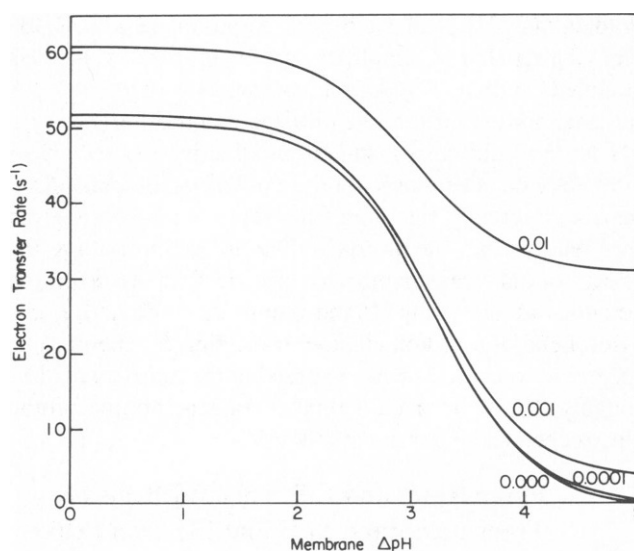


FIGURE 6  Electron transfer rate for the proton pump model (Fig. 3) as a function of the mitochondrial membrane pH gradient, for four different values of the electron leak rates. The parameters describing the pump are the same as those used in Fig. 4; the electron leak rates, again expressed as the ratio of isoergonic uncoupled and coupled electron transfer rates, are shown in the figure. As noted in the caption to Fig. 5, the isoergonic coupled electron transfer rate for this pump is 100 s$^{-1}$.

tions not shown) because the pump is then so inefficient that it functions mostly as an uncoupled electron leak.

The curves in Fig. 6 are similar to analogous curves calculated by Pietrobon and Caplan using a steady-state analysis of a pump that explicitly involved six states (34). In the language of linear nonequilibrium thermodynamics, the values of membrane $\Delta pH$ near the inflection points of these curves define the flow-controlling range of the force. The position of this flow-controlling range depends upon the rate constants chosen; in the present example they reflect the chosen value of $\Delta pK_a$ ($pK_a^{red} - pK_a^{ox} = 3.0$ units), and in the case of the simulations of Pietrobon and Caplan they are primarily determined by the equilibrium constant for a charge-translocating reaction step whose rate is influenced by transmembrane potential (34).

In Fig. 7, the rate and efficiency data of Figs. 5 and 6 are correlated. As one would expect, there is a trade-off between the efficiency and the rate. However, there is a wide range of rates over which the efficiency does not decrease very steeply, indicating that in these ranges a substantial gain in rate can be realized with relatively small sacrifice of efficiency. This is particularly true for the cases with nonzero electron leaks, and suggests that a real pump operating according to the schematic of Fig. 3 will ordinarily not operate at very high (>0.75) efficiency, because of the large loss in rate that this would entail, especially if its power output is an important consideration.

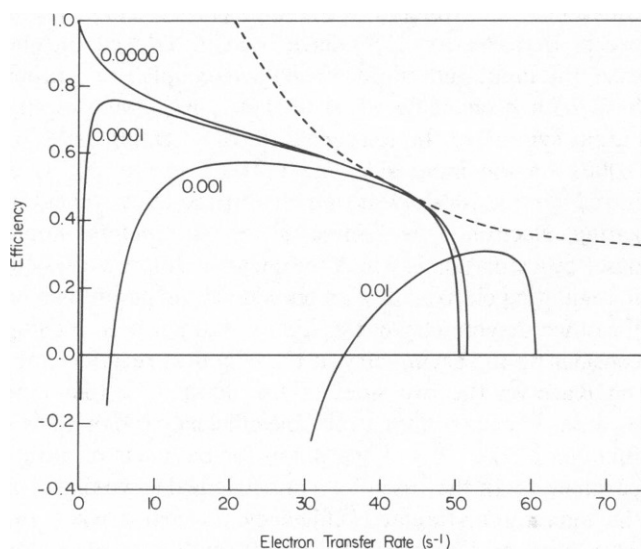Stucki (43) considered the effects of various degrees of



FIGURE 7 Efficiency vs. electron-transfer rate for the four-state pump of Fig. 3, for four different electron leak rates. The values of the other parameters used in the calculation are those specified in Table I. For a given leak rate, the position on the curve at which the pump actually operates is fixed by the applied membrane potential. Dashed line: A curve of constant power output. The point at which this curve is tangent to the rate vs. efficiency curve for leak rate 0.001 represents the conditions under which the pump with these parameters yields the maximum power output.

uncoupling upon a linear transducer, as measured by a variety of performance criteria including its output rate (proton pumping rate in the system currently under discussion), its output power, and the product of its power and its efficiency. This consideration of different performance criteria is important, because the energy-supplying systems in a cell are subject to selective pressure to maximize neither efficiency nor power output alone, but rather some compromise between the two. The ideal trade-off between efficiency and power will vary from tissue to tissue and will even vary temporally within a single tissue as its metabolic state changes. Stucki's analysis reaches the conclusion that various degrees of uncoupling (in the present context this would mean electron leakage) are actually beneficial in achieving optimal performance by the various criteria given above. This conclusion arises from the application of a constraint that the transducer will always operate at the maximum in its efficiency vs. load curves. We believe that this restriction is somewhat artificial. Since the operation of a transducer in a biologically advantageous fashion requires a compromise between maximization of efficiency and maximization of other performance criteria (e.g., power output and turnover rate), the most advantageous operation will not in general occur at the load (membrane potential) corresponding to maximal efficiency. If the transducer is very well coupled (as represented, for example, by the curves in Fig. 3 with the uncoupled/coupled rate ratio of 0.0001), and circumstances dictate that maximum power output is advantageous, it should not operate at the output force corresponding to the maximum in its attainable efficiency. By doing so, it would greatly decrease its turnover rate, and hence its power, relative to that achievable at lower output forces. It would instead operate near the point tangent to the dashed hyperbola (an "iso-power" curve) shown in Fig. 7, which corresponds to maximum power output. The tightly coupled pumps in Fig. 7 nevertheless have the capacity to operate at higher efficiencies, and correspondingly diminished power outputs, if this should become beneficial to the organism; this would entail an increase in the membrane $\Delta pH$ through much of its flow-controlling range. Possessing the capacity for more efficient operation will not by itself increase the likelihood that the transducer will actually operate farther away from its output optimum (as judged by whatever metabolic criterion one chooses) under any given metabolic circumstances. We therefore suggest, in contrast to the conclusion of Stucki (43), that in the present context of a single transducer (but see the discussion of cytochrome oxidase below) the more tightly coupled pumps can do everything that the less tightly coupled pumps can do, except more efficiently. (One exception should be noted: a poorly coupled transducer can generate heat in situations where this is desirable. However, specialized mechanisms involving controlled proton leakage through the mitochondrial membrane have evolved [63], evidently to effect independent metabolic regulation of heat production.)

As hinted above, the efficiency vs. rate curves in Fig. 7 can be used to determine the conditions under which the simple model transducer would function when its operation is subject to particular overall constraints. For example, the maximum power output of this transducer will occur where the efficiency vs. rate curves are tangent to a hyperbola defined by the equation: $(R_e-) (\eta) = P$, where $P$ is the maximum power output. The minimum rate of heat production will occur where the efficiency vs. rate curves are tangent to a hyperbola (not shown) defined by: $(R_e-) (1 - \eta) = Q$, where $Q$ is the minimum rate of heat production. The curves in Fig. 7 indicate that for a fairly broad range of electron leak rates, the condition for maximum power output corresponds to an efficiency in the neighborhood of 50% and a rate that is ~80% of the uncoupled rate. This suggests that under conditions where maximum power generation is required, this transducer will dissipate ~50% of its available free energy as heat. The occurrence of some reaction slip (uncoupled electron flow) will not have a significant effect on the power output of the transducer under these conditions, because most loss of free energy to heat production is not from the slip but from the net driving force for the coupled reactions. On the other hand, the minimum rate of heat generation, and the corresponding conditions, depend quite strongly upon the electron leak rates. Thus, the avoidance of slip is most important under resting conditions. Ideally, the relatively slow rate of respiration required to sustain the basal metabolic processes of the cell should fall near or to the right of the maxima of the curves in Fig. 7. Otherwise, the efficiency of electron transport would be greatly diminished, solely in order to achieve an inconsequential increase in the transmembrane proton gradient. This criterion for "impedance matching" is a much more restricted version (restricted because it pertains only to the resting condition of minimum metabolic load) of the general criterion which Stucki (43) suggests; as stated above, we consider it unlikely that a single impedance matching criterion applies to all of the diverse metabolic conditions that the transducer is likely to encounter.

## Optimization of $pK_a$s

Figs. 5–7 describe the effects of uncoupling processes and variations in membrane $\Delta pH$ upon the performance of a proton pump that is otherwise optimized. The same type of analysis may be used to examine the effect of changes in the pump parameters, e.g. $pK_a$s and reduction potentials, from their optimal values. In the upper panel of Fig. 8, the relationship between the $pK_a$s of the pump and its efficiency is displayed. In all cases, the thermodynamic linkage parameter $\Delta pK_a$ ($pK_a^{red} - pK_a^{ox}$) has been constrained to 3.0 units. Because the efficiency of pumping is closely related to the rate of turnover, a meaningful comparison of efficiency is not possible unless the turnover rate is also specified. In the top of Fig. 8, the turnover rate has therefore been constrained to particular levels by appropriate selection of the membrane $\Delta pH$. Three curves corresponding to three different turnover rates (10, 25, and 50 electrons transferred per second) are shown. In the lower panel of Fig. 8, the complementary comparison of turnover rate vs. the $pK_a$s of the pump is displayed. In this case, the efficiency has been constrained to particular values (0.4, 0.6, and 0.8) and for each efficiency value a corresponding curve relating turnover rate to $pK_a$s is shown. For a fixed rate of turnover, the efficiency of the pump is moderately sensitive to the values of the $pK_a$s between neutrality and the $pK_a$ value that enables maximum efficiency, and much more sensitive to the $pK_a$s at values above this (Fig. 8, top). The $pK_a$ values enabling maximum efficiency depend upon the turnover rate that is required. From the bottom panel of Fig. 8, it is evident that operation of the pump at near maximal rates depends rather critically upon appropriate selection of the $pK_a$s and that the optimal values for the pump $pK_a$s are determined by the efficiency that is required of the pump, reflecting the fact that the membrane $\Delta pH$ established at steady state depends upon the chosen efficiency. An examination of the calculations reveals that the maximum rate is achieved when the $pK_a$s are symmetrically disposed relative to the steady-state pH values on the two sides of the membrane (recall that the cytosol pH has been fixed at 7.0 and only the matrix pH allowed to vary). This is strictly a consequence of the symmetric character of the input and output states of the pump, which has been preserved by appropriate selection of the other input and output kinetic parameters.

The effect of asymmetric gating parameters is illustrated in Fig. 9, which uses the same parameters as Fig. 8 except that electron leaks have been introduced. In one case, the input and output uncoupled/coupled rate ratios have both been made equal to 0.001, preserving input/output symmetry. In a second case this "gating ratio" is 0.0001 on the input side and 0.01 on the output side, introducing a 100-fold asymmetry in the effectiveness of gating electron flow. These latter parameters would describe a situation in which the enzyme is more successful in regulating electron flow on one side of the pump than on the other. Asymmetry of this kind would not be surprising considering the asymmetry in the chemical reactions taking place on the two sides of the pump in cytochrome oxidase. The maximum attainable efficiency is plotted as a function of the $pK_a$s of the pump for both sets of gating parameters. In the case of asymmetric leaks, we find that the maximum attainable efficiency is greater when the $pK_a$s are not symmetrically placed with respect to the matrix and cytoplasm pH values. The corresponding analysis of electron transfer rate vs. $pK_a$ (plots not shown) indicates that the turnover rate still peaks near a symmetric $pK_a$ disposition and drops off approximately 10-fold when the $pK_a$s are more than 1.5 units removed from this. Nevertheless, the possibility that some asymmetry in gating efficiency exists suggests that the optimal $pK_a$s of the pump may be biased to values that would otherwise seem
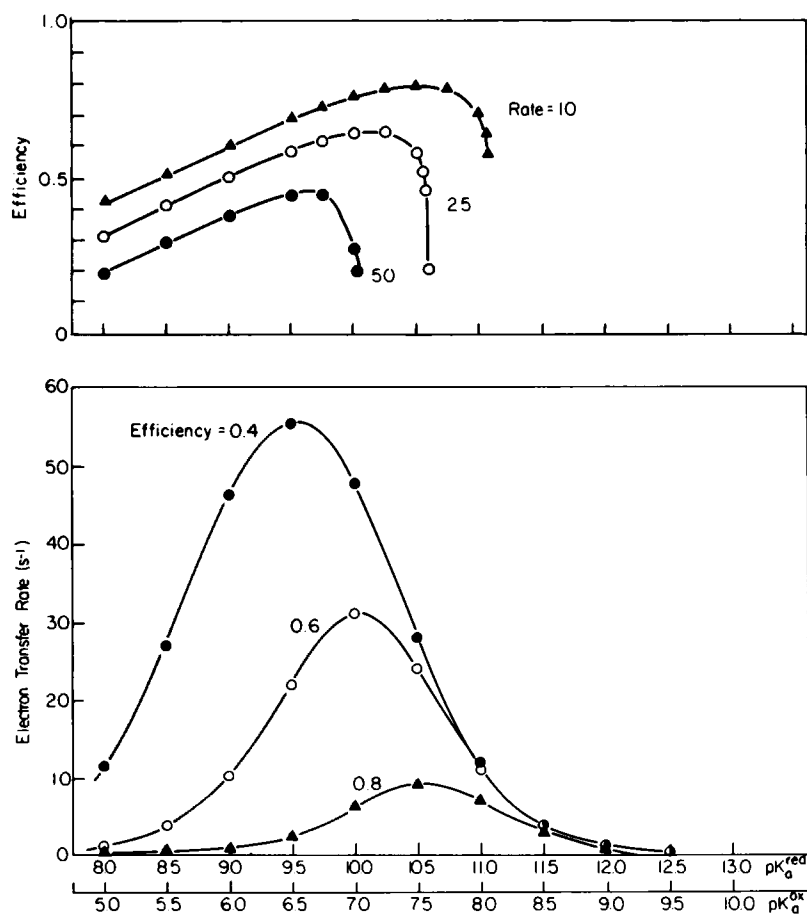
FIGURE 8  The efficiency of the pump at three different values of the electron transfer rate (*top*) and the electron transfer rate through the pump at three different values of the operating efficiency (*bottom*), as a function of the $pK_a$s of the pump. The parameters are the same as those used above in Figs. 5, 6, and 7, with a zero electron leak rate, except that $pK_a^{red}$ and $pK_a^{ox}$ have been varied while maintaining their difference constant at 3.0 units. The fixed values of turnover rate for the curves in the upper panel, and of efficiency for the curves in the lower panel, are indicated in the figure.
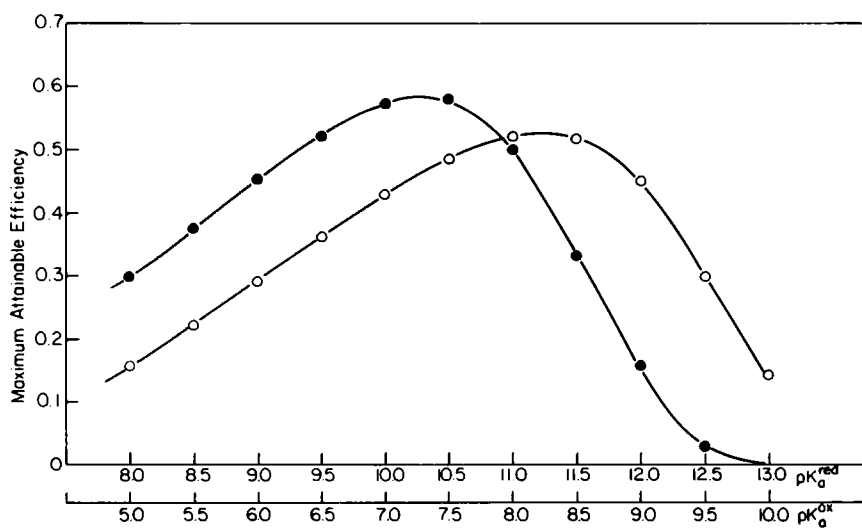


FIGURE 9  The maximum attainable efficiency of the four-state pump as a function of the $pK_a$s of the pump, for two different sets of electron leak parameters (for leaks equal to zero, the maximum attainable efficiency is always 1.0). Parameters are the same as in Fig. 7, except that two sets of electron leaks have been introduced: a symmetric case where input and output leak ratios are both equal to 0.001 (closed circles), and an asymmetric case where input and output leak ratios are equal to 0.0001 and 0.01, respectively (open circles).

surprisingly high or low. In the present example, $pK_a$s of 8.5 and 11.5 would be best for efficiency, but electrochemical titrations in the pH range between 6.0 and 8.0 (i.e., below the pump $pK_a$s) would not reveal a very pronounced pH dependence of the pump's reduction potential (see Fig. 2).

If there is an appreciable electrical potential across the membrane, as is expected (50–53), and if the pumping site is connected to the solution phases via proton channels that traverse a portion of this transmembrane potential, then the effective proton activities at the pump will be different from the bulk solution proton activities. This is because a proton channel or "well" (64) can transduce the electrical potential difference into a chemical potential difference, assuming proton conduction is sufficiently facile (64). This effect would change the optimal $pK_a$s of the pump. For example, if the transmembrane electrostatic potential $\Delta\varphi$ is 120 mV and if the pump is connected to the matrix by a proton channel that traverses this entire potential, the effective pH at the input of the pump will be 2.0 units higher than the matrix pH. (In this example, the pH on the output side will remain the same.) For a fixed thermodynamic linkage parameter $\Delta pK_a$, the optimal $pK_a$s in an analysis like that of Fig. 8 would both be increased by 1.0 unit (preserving input/output symmetry). Thus an asymmetric placement of the pumping site in the transmembrane potential profile would, like asymmetric effectiveness in gating, lead to optimal $pK_a$s biased away from neutrality.

The effect of varying the pump $pK_a$s upon the maximum attainable transmembrane proton electrochemical potential (the static head condition, in the language of linear irreversible thermodynamics) was also examined. These calculations (not shown) indicated that the static head proton gradient is determined primarily by the isoergonic uncoupled/coupled electron transfer rate ratio, and is to a surprising degree insensitive to the $pK_a$s of the pump and to the magnitude of thermodynamic linkage between oxidoreduction and protolysis (cf. below). This insensitivity is at least in part a consequence of the present assumption that the gating of protons is perfect. If proton leaks involving the vertical segments of the cycle in Fig. 3 were introduced, the static head $\Delta$pH would depend more sensitively upon the pump $pK_a$s.

## The Role of Thermodynamic Linkage

It is instructive to examine the role of thermodynamic linkage between oxidoreduction and protolysis, as measured by the quantity $\Delta pK_a$ ($pK_a^{red} - pK_a^{ox}$). It is sometimes assumed that significant (comparable in magnitude to the transmembrane proton electrochemical potential) linkage of this kind is essential to achieve the necessary rapid turnover rates (12, but see also reference 23). In Fig. 10, rate vs. efficiency plots are shown for several different values of $\Delta pK_a$, for a pump driven by an available free energy of 300 mV (corresponding to a maximum attain-

able membrane $\Delta$pH of 5 units, given perfect efficiency). Two cases are presented: perfect gating (Fig. 10 $A$) and gating ratios of 0.001 (Fig. 10 $B$). It is seen in Fig. 10 $A$ that for a given electron transfer rate only a small (10–15%) loss in efficiency accompanies the decrease in thermodynamic linkage from $\Delta pK_a$ = 4 to $\Delta pK_a$ = 2. In the efficiency range around 0.7, which as suggested above may be the optimal range of operation when output power is important, the decrease in thermodynamic linkage from 4.0 units to 2.0 units causes only about a threefold decrease in electron transfer rate. Further decreasing the linkage to only 1.0 units decreases the efficiency by approximately an additional 15%, or the rate by an additional factor of 3. In Fig. 10 $B$, where electron leaks have been introduced, even more striking behavior is observed: A decrease in thermodynamic linkage from 4.0 units to 2.0 units decreases peak efficiency by only ~8% while actually increasing the rate of electron transfer at many efficiency values. Thus the pumps with less thermodynamic linkage exhibit greater flexibility with respect to the range of rates and power outputs that they can achieve. Among those shown in Fig. 10, the pumps with $\Delta pK_a$ = 2 are able to generate most power, again by operating at ~50% efficiency.
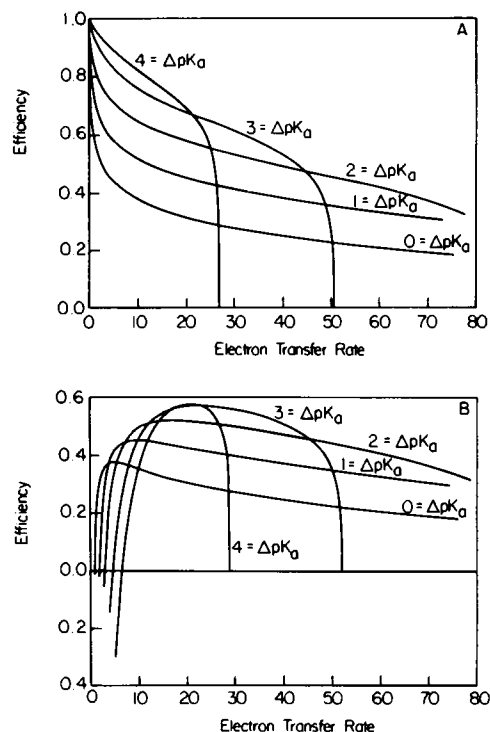


Figure 10 Efficiency vs. rate plots for four-state proton pumps with different degrees of thermodynamic linkage, measured as the difference betwen the $pK_a$s of the oxidized and reduced pumps. Parameters are the same as in Figs. 4, 5, and 6, except that $pK_a^{ox}$ was fixed at 7, and the thermodynamic coupling parameters $E_H^o$, $E_L^o$, and $pK_a^{red}$ have been varied in the following manner: $\Delta pK_a$ = 4: $pK_a^{red}$ = 11, $E_H^o$ = 520 mV, $E_L^o$ = 280 mV; $\Delta pK_a$ = 3: $pK_a^{red}$ = 10, $E_H^o$ = 490 mV, $E_L^o$ = 310 mV; $\Delta pK_a$ = 2: $pK_a^{red}$ = 9, $E_H^o$ = 460 mV, $E_L^o$ = 340 mV; $\Delta pK_a$ = 1: $pK_a^{red}$ = 8, $E_H^o$ = 430 mV, $E_L^o$ = 370 mV; $\Delta pK_a$ = 0: $pK_a^{red}$ = 7, $E_H^o$ = $E_L^o$ = 400 mV. ($A$) No electron leaks. ($B$) Input and output electron leak ratios of 0.001.

The most important reason for these results is the connection between electron transfer rate and electron transfer exergonicity which has been incorporated in the analysis. While a decrease in thermodynamic linkage causes the $pK_a$s of the pump to be less closely matched to the proton input and output environments, it also causes the rate constants for the desired (coupled) electron transfers to increase because these processes become more exergonic and the rate constants for the uncoupled electron transfers to decrease because these processes become less exergonic (Fig. 11). As described earlier, these effects must be considered, because a correlation of electron transfer rate and exergonicity is anticipated on the basis of both theory (22, 27) and experiment (25). This argument does not overlook the fact that other factors are important in determining electron transfer rates; these factors are incorporated in the isoergonic electron transfer rates that are used to express the overall effectiveness of the gating of electron flow. In the examples simulated in Fig. 10 B, these other factors are assumed to favor the coupled electron transfers relative to the uncoupled ones by a fairly large factor (1,000); this factor is the same for all of the curves.

As the thermodynamic linkage parameter $\Delta pK_a$ is made smaller, the observed pH dependence of the reduction potential of the pump will also diminish, especially if the $pK_a$s of the pump are not symmetrically disposed about 7.0. For example, with $pK_a$s of 8.0 and 10.0, a fairly weak pH dependence would be observed below pH 8. A pump

with these $pK_a$s may be optimal given significant asymmetry of the kinds described above, and certainly appears acceptable in view of the comparisons shown in Fig. 10.

The thermodynamic linkage discussed here should not be confused with the degree of coupling $q$ of linear nonequilibrium thermodynamics, or any other parameter that describes the effectiveness of coupling between input and output processes. The thermodynamic linkage under discussion reflects the energetics of the reaction path as determined by $pK_a$s (or, equivalently, reduction potentials), not the degree to which the electron transfers are "linked" to proton pumping through, for example, a flow ratio. Hence our suggestion that decreased thermodynamic linkage can lead to enhanced performance under some circumstances is entirely different from Stucki's conclusion, discussed above, that partial uncoupling of one flow from the other can enhance performance.

## Summary of the Steady-State Analysis

The analysis of the four-state model shows that the consideration of electron leak processes leads to some novel conclusions. It reveals at least two plausible mechanisms whereby a pump of this type may not exhibit a pronounced pH dependence of its reduction potential. These are: First, asymmetrical disposition of the pump $pK_a$s, which is required for optimal efficiency in situations having an asymmetry in the input/output gating efficiencies or in the placement of the pump site in the transmembrane potential profile; and second, a smaller thermodynamic linkage than would otherwise be expected, which still leads to performance that is comparable to a pump with greater linkage because the electron transfer rates correlate with reaction exergonicites.

A second conclusion arising from the steady-state analysis is that efficient operation of a redox-linked proton pump of this kind requires quite stringent control of electron flow. Specifically, for a pump described by the parameters in Fig. 3, which are intended to approximate cytochrome $c$ oxidase, a gating ratio of 0.001 or smaller (measured as the ratio of the uncoupled and coupled isoergonic electron transfer rates) would be desirable. The isoergonic electron transfer rates depend upon intersite distance, the nature of the intervening material, and the reorganizational energies; changing any one of these must necessarily involve some structural change at or near the pump site (for example, a 1,000-fold enhancement of electron transfer rate would require an ~5 Å decrease in intersite distance, according to one estimate [15]).

### DOES ELECTRON TRANSFER SLIP ACTUALLY OCCUR IN MITOCHONDRIAL OXIDATIVE PHOSPHORYLATION?

The possibility of molecular slip (uncoupling of transduction at the molecular level, for example by electron leakage of the kind described above) in mitochondrial free energy transduction, and the need for various forms of gating,
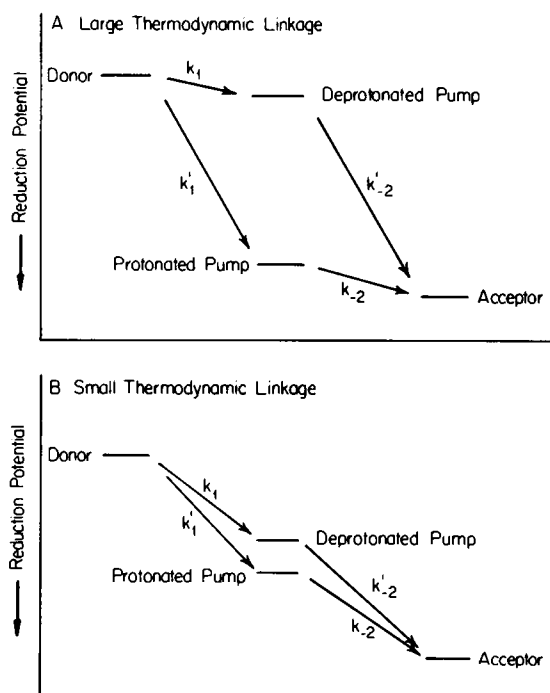


FIGURE 11 The effect of changing the degree of thermodynamic linkage upon the various electron transfer exothermicities. The uncoupled electron transfers ($k_1'$ and $k_2'$) are always more exothermic than the coupled ones ($k_1$ and $k_2$); as the thermodynamic linkage increases, this difference in exothermicities increases.

have been noted before (12, 42, 43, 45, 46, 65–67). The implications of electron transfer slip have not, however, been explored in terms of its likely mechanisms and its consequences for the mechanisms of redox-linked proton pumping. The occurrence of significant reaction slip has sometimes even been dismissed as unlikely (1). This neglect of slip would be justified if it could be shown that mitochondrial free energy transduction is very nearly 100% efficient in State 4 (the fully membrane-energized state), as has sometimes been supposed (68, 69).

The efficiency of respiring mitochondria has been estimated by combining measurements of the operating potentials of the electron transport components and the maximum attainable phosphorylation potential in resting (State 4) mitochondria (68) with measurements of the number of ATP molecules synthesized per oxygen atom consumed (the P/O ratio) in phosphorylating (State 3) mitochondria (70, 71). On this basis, it has been claimed (68, 69) that the electron transfer reactions are very nearly at thermodynamic equilibrium with the phosphorylation reactions, so that $\Delta G$ for the coupled reactions approaches zero, implying close to 100% free energy conservation efficiency. The validity of this method is questionable, as others have noted (43–46), because it involves the comparison of thermodynamic quantities with rates measured away from equilibrium, assuming in particular that the P/O ratio is unchanged on going from State 3 to State 4. Measurements of the P/O ratio under a range of conditions intermediate between States 3 and 4 (72) show that the P/O ratio actually decreases by approximately twofold as State 4 is approached. Hence the occurrence of significant slip cannot be dismissed on the basis of the classical supposition of very high efficiency. Investigations of oxidative phosphorylation that were analyzed in terms of irreversible thermodynamics, which explicitly recognizes the nonequilibrium character of the process, indicate that the mitochondrial proton pumps are probably not perfectly coupled (45, 46).

Sorgato et al. (73–75) and Pietrobon et al. (66, 67) have obtained experimental evidence for reaction slip on the molecular level in the mitochondrial ATPase (73, 66) and sites of electron transfer-driven proton translocation (74, 67). Both groups have examined the rates of electron transfer and ATP synthesis in the presence of inhibitors of electron transport, and have correlated these rates with the steady-state transmembrane proton electrochemical potentials which are maintained. Sorgato et al. interpreted their results in terms of a variable membrane conductance (73, 74), while acknowledging the alternative possibility of reaction slip (75). Pietrobon et al. have concluded that reaction slip is the only viable explanation, and in the case of electron transfer-driven proton pumping have also obtained evidence that the reaction slip involves the electron transfer steps rather than leakage of protons through the pump (66, 67, but cf. reference 76). Their conclusions

suggest that the emphasis placed upon the regulation of electron movements in the present analysis is appropriate. It has been stated that it is hard to visualize a free energy transducer that is designed to lose free energy as heat via molecular-level slip (1). The considerations outlined above indicate that slippage paths in redox-driven proton translocation are readily envisioned, and in fact such slip may not be so much a consequence of design as of difficulty in achieving the stringent control over electron movements that is required to avoid it.

## CYTOCHROME c OXIDASE

Proton pumping by cytochrome c oxidase has been the subject of numerous investigations (4) involving both measurement of the proton/electron stoichiometry (40, 41) and measurement of thermodynamic (77, 78) or spectroscopic (79) properties that might bear on the mechanism of proton pumping. In particular, a moderate pH dependence of the reduction potential of $Fe_a$ has been observed (80, 5, 7). This observation has been cited as evidence that $Fe_a$ performs the proton pumping function (12). In the light of the above discussion, it is clear that a pH-dependent reduction potential is not required for reasonably efficient proton pumping. Moreover, the observed dependence is maximally only $-30$ mV/pH unit (80, 7), and is even less steep at pH values above 7, which are relevant to the mitochondrial matrix (7). These observations are not consistent with a mechanism of proton pumping in which $pK_a^{ox}$ is considerably less than 7 and $pK_a^{red}$ is considerably greater than 7 (Fig. 2). If the intrinsic pH dependence of the $Fe_a$ reduction potential is even less than this ($-8$ mV/pH unit), as recent spectroelectrochemical measurements on the carbon monoxide inhibited enzyme indicate (5), then protonation is not very tightly coupled to reduction of $Fe_a$ and the pH effect on the reduction potential may involve a protonating site that is relatively remote from the iron center. The pH dependence of the $Fe_a$ reduction potential is thus not a sound basis for concluding that $Fe_a$ is the proton pump. The other site that has been considered as a possible proton pump is $Cu_A$ (10). The reduction potential of this site is weakly if at all pH-dependent (77); the present analysis has shown that this observation is not inconsistent with a proton pumping function.

Estimates of the efficiency of free energy conservation by cytochrome c oxidase are complicated by the fact that the various intermediates of dioxygen reduction produced at the $Fe_{a_3}/Cu_B$ site of this enzyme are chemically very different and hence likely to have different standard reduction potentials. The rates of electron transfer to this site may therefore be different at each of the steps in dioxygen reduction. In one estimate of the efficiency of free energy conservation by cytochrome c oxidase (1), a single effective reduction potential, that of the overall

$O_2/H_2O$ couple, was used, and an efficiency estimate of 90% was obtained, based on the assumption of unit stoichiometry (i.e., no slip) under highly membrane-energized (State 4) conditions. The stoichiometry of one proton pumped per electron transferred is based upon measurements of proton pumping in mitochondria (81) or in vesicles (40) in which the transmembrane electrical potential was mostly discharged by uncoupling agents. Hence this efficiency estimate suffers from the same difficulty described above, namely the use of stoichiometries measured kinetically in combination with thermodynamic quantities measured under conditions closer to equilibrium. The actual stoichiometry of proton pumping by cytochrome oxidase could be significantly less than one; when an appreciable membrane potential is allowed to develop, the measured stoichiometries decrease significantly (41).

It was stated above that the performance of a single transducer will be enhanced by minimizing reaction slip. The situation is more complicated, however, when one considers the aggregate behavior of a system in which a series of transducers contribute to the overall performance of the system (as in mitochondrial oxidative phosphorylation) or of one in which a series of transduction events with different performance properties must occur sequentially. Cytochrome oxidase falls into the latter category, since its turnover cycle really involves four chemically distinct transduction steps in temporal series. We have suggested (82, 83) that some reaction slip may be advantageous at steps in dioxygen reduction which would otherwise be slow, either because they are less exergonic or because they involve large reorganizational energies. Stalling electron transfer at one relatively difficult step within cytochrome oxidase would also arrest energy conservation at all of the other sites in the respiratory chain, with clearly adverse consequences. This situation is somewhat analogous to that of the salt pump examined theoretically by Caplan and Essig (44), which consists of an active cation transporter operating in parallel with a passive leak that permits the passage of both anions and cations. While the existence of the passive leak decreases the efficiency of cation pumping, it enables the anion translocation step, which is also essential to the overall process of salt transfer. The optimal strategy for cytochrome oxidase might be to make coupling as tight as possible at the pumping site, but to employ in addition a second independently controlled electron transfer pathway that completely bypasses the proton pump. Recently, evidence for multiple routes of electron transfer through the enzyme has been obtained, in investigations of electron transfer in a chemically modified derivative of the enzyme at room temperature (82) and the native enzyme at low temperature (83).

The importance of effective regulation of electron flow has been demonstrated. This regulation is likely to involve significant structural changes at the pumping site. It is noteworthy that localized molecular mechanisms for coupling protonation to the gating of electrons, such as ligand protonation, ligand exchange, and metal ion movement, are more readily envisioned occurring at a metalloprotein copper center than at a heme iron. The axial ligands of $Fe_a$ are almost certainly neutral histidyl imidazoles in both the oxidized and reduced states of the iron (83, 84), and the coordination geometry changes accompanying the reduction of $Fe_a$ are expected to be small, since the iron is low-spin in both redox states. In contrast, there is no evidence against a change in the identity or geometry of the coordinating ligands upon reduction of $Cu_A$. Substantial changes in the coordination geometry of $Cu_A$ upon reduction would not be surprising, since copper exhibits very different preferred geometries in its cuprous and cupric states (86). The electron transfers into and out of $Fe_a$ are likely to take place via the heme macrocycle (87, 88), which is not expected to undergo large movements in relation to the protein as a whole. Hence the gating of electron flow through $Fe_a$ would probably involve conformational changes at the formyl (8) and/or vinyl groups on the periphery of the macrocycle, or more gross protein conformational changes that change the alignment of electron-conducting groups between the heme and its electron-transfer partners. The effectiveness of gating by these mechanisms cannot be assessed precisely with presently available theory, but would be limited by the occurrence of electron transfer via more than one locus on the heme edge.

In summary, the present analysis weakens the traditional arguments that implicate $Fe_a$ as the proton pump in cytochrome oxidase, while introducing new considerations that suggest that pumping mechanisms that involve $Cu_A$ and that explicitly incorporate gating of electron flow can be formulated readily. However, no compelling arguments for one or the other site may be advanced on the basis of these ideas alone, and reliable selection between the alternatives must await more information from experiment. Studies on the structure of the reduced $Cu_A$ and $Fe_a$ sites and a fairly detailed elucidation of the nature of the steady state (with respect to the levels of $Fe_a$ and $Cu_A$ reduction) and its response to membrane energization would be helpful in this regard. Also, electron transfer slip deserves direct study, for example by measurements of the proton permeability of vesicles containing cytochrome oxidase poised at various levels of reduction but prevented from undergoing net turnover, either by the absence of substrate $O_2$ or by complexation with inhibitors.

## APPENDIX

### Solution of the Steady-State Equations for the Four-State Proton Pump

We require the steady-state concentrations of each of the four pump species in the reaction scheme given in Fig. 3. First, the various species

concentrations are defined

$$[D_{red}] = r_1 \quad [P_{ox}] \quad = \quad P_o \quad [H_m^+] = H_m^+$$

$$[D_{ox}] = o_1 \quad [P_{red}] \quad = \quad P_r \quad [H_c^+] = H_c^+$$

$$[A_{red}] = r_2 \quad [P_{ox} \cdot H^+] = P_o \cdot H^+$$

$$[A_{ox}] = o_2 \quad [P_{red} \cdot H^+] = P_r \cdot H^+.$$

Total concentration of pumping sites $= P_T$.

The steady-state rate equations are

$$P_o + P_r + P_o \cdot H^+ + P_r \cdot H^+ = P_T \qquad (A1)$$

$$(k_{oa}H_c^+ + k_1r_1)P_o - (k'_{-2}o_2 + k_{-1}o_1)P_r$$
$$- (k_{od})P_o \cdot H^+ = 0 \quad (A2)$$

$$-(k_1r_1)P_o + (k'_{-2}o_2 + k_{-1}o_1 + k_{ra}H_m^+)P_r$$
$$- (k_{rd})P_r \cdot H^+ = 0 \quad (A3)$$

$$-(k_{oa}H_c^+)P_o + (k_{od} + k_2r_2 + k'_1r_1) P_o \cdot H^+$$
$$- (k_{-2}o_2)P_r \cdot H^+ = 0. \quad (A4)$$

These four equations are used to define the matrix equation

$$\begin{bmatrix} C_{11} & C_{12} & C_{13} & C_{14} \\ C_{21} & C_{22} & C_{23} & 0 \\ C_{31} & C_{32} & 0 & C_{34} \\ C_{41} & 0 & C_{43} & C_{44} \end{bmatrix} \begin{bmatrix} P_o \\ P_r \\ P_o \cdot H^+ \\ P_r \cdot H^+ \end{bmatrix} = \begin{bmatrix} P_T \\ 0 \\ 0 \\ 0 \end{bmatrix}$$

thereby defining the $C_{nm}$'s.

Rows 2-4 of the matrix may be manipulated to give all species concentrations relative to $P_o$. The results of these manipulations are

$$P_r \cdot H^+ = \frac{C_{21}C_{32}C_{43} - C_{31}C_{22}C_{43} - C_{23}C_{41}C_{32}}{C_{43}C_{22}C_{34} + C_{44}C_{32}C_{23}} \cdot P_o \quad (A5)$$

$$P_o \cdot H^+ = \frac{C_{31}C_{44}C_{22} - C_{34}C_{41}C_{22} - C_{32}C_{21}C_{44}}{C_{43}C_{22}C_{34} + C_{44}C_{32}C_{23}} \cdot P_o \quad (A6)$$

$$P_r = \frac{C_{41}C_{23}C_{34} - C_{43}C_{21}C_{34} - C_{44}C_{31}C_{23}}{C_{43}C_{22}C_{34} + C_{44}C_{32}C_{23}} \cdot P_o. \quad (A7)$$

Inserting these expressions into the expressions for the rates of proton pumping and electron transfer (Eqs. 1 and 2), we obtain

$$R_{H^+} = \left\{ k_{ra}H_m^+ \left( \frac{C_{41}C_{23}C_{34} - C_{43}C_{21}C_{34} - C_{44}C_{31}C_{23}}{C_{43}C_{22}C_{34} + C_{44}C_{32}C_{23}} \right) \right.$$
$$\left. - k_{rd} \left( \frac{C_{21}C_{32}C_{43} - C_{31}C_{22}C_{43} - C_{23}C_{41}C_{32}}{C_{43}C_{22}C_{34} + C_{44}C_{32}C_{23}} \right) \right\} \cdot P_o. \quad (A8)$$

and

$$R_{e^-} = \left\{ k_1r_1 + k'_1r_1 \left( \frac{C_{31}C_{44}C_{22} - C_{34}C_{41}C_{22} - C_{32}C_{21}C_{44}}{C_{43}C_{22}C_{34} + C_{44}C_{32}C_{23}} \right) \right.$$
$$\left. - k_{-1}o_1 \left( \frac{C_{41}C_{23}C_{34} - C_{43}C_{21}C_{34} - C_{44}C_{31}C_{23}}{C_{43}C_{22}C_{34} + C_{44}C_{32}C_{23}} \right) \right\} \cdot P_o. \quad (A9)$$

The quotient of these is the flow ratio (the effective reaction stoichiometry)

$$X = \frac{R_{H^+}}{R_{e^-}}$$

$$= \frac{k_{ra}H_m^+(C_{41}C_{23}C_{34} - C_{43}C_{21}C_{34} - C_{44}C_{31}C_{23})}{\{k_1r_1(C_{34}C_{43}C_{22} + C_{32}C_{23}C_{44})}$$
$$\frac{- k_{rd}(C_{21}C_{32}C_{43} - C_{31}C_{22}C_{43} - C_{23}C_{41}C_{32})}{+ k'_1r_1(C_{31}C_{44}C_{22} - C_{34}C_{41}C_{22} - C_{32}C_{21}C_{44})} \quad (A10)$$
$$- k_{-1}o_1(C_{41}C_{23}C_{34} - C_{43}C_{21}C_{34} - C_{44}C_{31}C_{23})\}.$$

After replacement of the $C_{nm}$'s by the appropriate rate constants and simplification, this becomes

$$X = \frac{\begin{aligned} &k_{ra}H_m^+k_{-2}o_2k_1r_1k_{od} \\ &- k_{rd}k_{oa}H_c^+ \cdot (k'_{-2}o_2 + k_{-1}o_1)(k_2r_2 + k'_1r_1)\end{aligned}}{\begin{aligned} &\{k_1r_1[k_{rd}k'_{-2}o_2(k_{od} + k_2r_2 + k'_1r_1) \\ &+ k_{od}k_{-2}o_2(k'_{-2}o_2 + k_{ra}H_m^+)] \\ &- k_{-1}o_1k_2r_2k_{oa}H_c^+k_{rd} + k'_1r_1[k_{rd}k_{oa}H_c^+k'_{-2}o_2 \\ &+ k_{ra}H_m^+k_1r_1k_{-2}o_2 \\ &+ (k'_{-2}o_2 + k_{-1}o_1 + k_{ra}H_m^+)(k_{oa}H_c^+k_{-2}o_2)]\}.\end{aligned}}$$

(A11)

This expression is equivalent to Eq. 5.

The other important quantity is the electron tranfer rate per pump site, $R_{e^-}/P_T$. This is obtained from Eq. A9 above by inserting the appropriate rate constants in place of the $c_{nm}$'s. The resulting equation is

$$\frac{R'_e}{P_T} = \frac{\begin{aligned} &\{k_1r_1[k_{rd}k'_{-2}o_2(k_{od} + k_2r_2 + k'_1r_1) \\ &+ k_{od}k_{-2}o_2(k'_{-2}o_2 + k_{ra}H_m^+)] - k_{-1}o_1k_2r_2k_{oa}H_c^+k_{rd} \\ &+ k'_1r_1[k_{rd}k_{oa}H_c^+k'_{-2}o_2 + k_{ra}H_m^+k_1r_1k_{-2}o_2 \\ &+ (k'_{-2}o_2 + k_{-1}o_1 + k_{ra}H_m^+)(k_{oa}H_c^+k_{-2}o_2)]\}\end{aligned}}{\begin{aligned} &\{[(k_{od} + k_{oa}H_c^+)k_{-2}o_2 + (k_2r_2 + k'_1r_1)k_{oa}H_c^+] \\ &\cdot (k'_{-2}o_2 + k_{-1}o_1 + k_{ra}H_m^+) \\ &+ [k_{rd}(k'_{-2}o_2 + k_{-1}o_1 + k_1r_1) + k_{ra}H_m^+k_1r_1] \\ &\cdot k_{od} + k_2r_2 + k'_1r_1) \\ &+ k_{oa}H_c^+k_{rd}(k_2r_2 + k'_1r_1 + k'_{-2}o_2 + k_{-1}o_1) \\ &+ k_1r_1k_{-2}o_2(k_{ra}H_m^+ + k_{od})\}.\end{aligned}}$$

(A12)

This expression is equivalent to Eq. 4.

The overall efficiency of the pump was calculated from the flow ratio and the membrane potential according to Eq. 4 in the text.

For all calculations, it was assumed that $2.303RT/\mathcal{F} = 60$ mV, for simplicity. (This is used in relating membrane potentials given in pH units to reduction potentials in mV; e.g., a membrane pH gradient of 5 units corresponds to a potential difference of 300 mV.)

An important element in the simulations of proton pump performance is the incorporation of a connection between electron transfer exergonicity and rate. In accordance with the considerations outlined in the text, electron transfer rate constants were adjusted according to

$$k = k_{iso} (e^{-\Delta G^\circ/2RT}),$$

where $k_{iso}$ is an isoergonic electron transfer rate, which is either specified directly (in the case of the "leaks") or fixed by the electron transfer rate products EP1 and EP2 (the products of the forward and backward rate constants), and $\Delta G^\circ$ is the standard free-energy change of the electron transfer reaction.

The equations describing the steady state behavior of systems of

reactions like that in Fig. 1, and particularly of more complex reaction schemes, may also be obtained with a minimum of labor by applying a set of rules described by Hill (89).

## REFERENCES

1. Wikström, M., and K. Krab. 1980. Respiration-linked $H^+$ translocation in mitochondria: stoichiometry and mechanism. *Curr. Top. Bioenerg.* 10:51–101.
2. Maloney, P. C. 1982. Energy Coupling to ATP Synthesis by the Proton-Translocating ATPase. *J. Membr. Biol.* 67:1–12.
3. Mitchell, P. 1961. Coupling of phosphorylation to electron and hydrogen transfer by a chemi-osmotic type of mechanism. *Nature (Lond.).* 191:144–148.
4a. Wikström, M., and K. Krab. 1979. Proton-Pumping Cytochrome c Oxidase. *Biochim. Biophys. Acta.* 549:177–222.
4b. Wikström, M. 1984. Pumping of Protons from the Mitochondrial Matrix by Cytochrome Oxidase. *Nature (Lond.).* 308:558–560.
5. Ellis, W. R., H. Wang, D. F. Blair, H. B. Gray, and S. I. Chan. 1986. Spectroelectrochemical studies of the cytochrome a site in carbon monoxide inhibited cytochrome c oxidase. *Biochemistry.* 25:161–167.
6. Wang, H., D. F. Blair, W. R. Ellis, Jr., H. B. Gray, and S. I. Chan. 1986. Temperature dependence of the reduction potential of $Cu_A$ in carbon monoxide inhibited cytochrome c oxidase. *Biochemistry.* 25:167–171.
7. Blair, D. F., W. R. Ellis, Jr., H. Wang, H. B. Gray, and S. I. Chan. 1986. Spectroelectrochemical study of cytochrome c oxidase: pH and temperature dependences of the cytochrome potentials. Characterization of site-site interactions. *J. Biol. Chem.* In press.
8. Babcock, G. T., and P. M. Callahan. 1983. Redox-linked hydrogen bond strength changes in cytochrome a: implications for a cytochrome oxidase proton pump. *Biochemistry.* 22:2314–2319.
9. Wikström, M., K. Krab, and M. Saraste. 1981. Proton-translocating cytochrome complexes. *Annu. Rev. Biochem.* 50:623–655.
10. Chan, S. I., D. F. Bocian, G. W. Brudvig, R. H. Morse, and T. H. Stevens. 1979. The nature of the "visible" copper in cytochrome c oxidase. *In* Cytochrome Oxidase. T. E. King, Y. Orii, B. Chance, and K. Okunuki, editors. Elsevier/North-Holland Biomedical Press (Amsterdam). 177–188.
11. Papa, S. 1976. Proton translocation reactions in the respiratory chains. *Biochim. Biophys. Acta.* 456:39–84.
12. Wikström, M., K. Krab, and M. Saraste. 1981. Cytochrome oxidase: a synthesis. Academic Press, London. 198 pp.
13. Casey, R. P., M. Thelen, and A. Azzi. 1980. Dicyclohexylcarbodiimide binds specifically and covalently to cytochrome c oxidase while inhibiting its $H^+$-translocating activity. *J. Biol. Chem.* 255:3994–4000.
14. Nagle, J. F., and M. Mille. Molecular models of proton pumps. *J. Chem. Phys.* 74(2):1367–1372.
15. Hoppe, J., and W. Sebald. 1984. The Proton Conducting $F_o$-Part of Bacterial ATP Synthases. *Biochim. Biophys. Acta.* 768:1–27.
16. Okamoto, H., N. Sone, H. Hirata, M. Yoshida, and Y. Kagawa. 1977. Purified proton conductor in proton translocating adenosine triphosphatase of a thermophilic bacterium. *J. Biol. Chem.* 252:6125–6131.
17. Nelson, N. 1980. Proton channels in chloroplast membranes. *Ann. NY. Acad. Sci.* 358:25–35.
18. Schneider, E., and K. Altendorf. 1984. The proton-translocating portion $(F_o)$ of the *E. coli* ATP Synthase. *Trends. Biochem. Sci.* 9:51–53.
19. Kagawa, Y. 1978. Reconstitution of the energy transformer, gate, and channel subunit reassembly, crystalline ATPase and ATP synthesis. *Biochim. Biophys. Acta.* 505:45–93.
20. DeVault, D. 1971. Energy transduction in electron transport. *Biochim. Biophys. Acta.* 225:193–199.
21. Hopfield, J. J. 1982. The mechanism of electron transfer in the electron transport chain. *In* Oxidases and Related Systems. T. E. King, editor. Pergamon Press, Oxford. 35–49.
22. Hopfield, J. J. 1974. Electron transfer between biological molecules by thermally activated tunneling. *Proc. Natl. Acad. Sci. USA.* 71:3640–3644.
23. Malmström, B. 1985. Cytochrome c oxidase as a proton pump. A transition-state mechanism. *Biochim. Biophys. Acta.* 811:1–12.
24. Marcus, R. A., and N. Sutin. 1985. Electron transfer in chemistry and biology. *Biochim. Biophys. Acta.* 811:265–322.
25. Meyer, T. E., C. T. Przysiecki, J. A. Watkins, A. Bhattacharyya, R. P. Simonsden, M. A. Cusanovich, and G. Tollin. 1983. Correlation between rate constant for reduction and redox potential as a basis for systematic investigation of reaction mechanisms of electron transfer proteins. *Proc. Natl. Acad. Sci. USA.* 80:6740–6748.
26. Dutton, P. L. 1978. Redox potentiometry: determination of midpoint potentials of oxidation-reduction components of biological electron-transfer systems. *Methods Enzymol.* 54:411–435.
27. Marcus, R. A. 1979. Electron transfer and tunneling in chemical and biological systems. *In* Light-Induced Charge Separation in Biology and Chemistry. H. Gerischer and J. J. Katz, editors. Weinheim (New York). 15–43.
28. Winkler, J. R., D. G. Nocera, K. M. Yocom, E. Bordignon, and H. B. Gray. 1982. Electron-transfer kinetics of pentaammineruthenium(III) (histidine-33)-ferricytochrome c. Measurement of the rate of intramolecular electron transfer between redox centers separated by 15 Å in a protein. *J. Am. Chem. Soc.* 104:5798–5800.
29. Margalit, R., N. M. Kostic, C.-M. Che, D. F. Blair, H.-j. Chiang, I. Pecht, J. B. Shelton, J. R. Shelton, W. A. Schroeder, and H. B. Gray. 1984. Preparation and characterization of pentaammineruthenium-(histidine-83) azurin: Thermodynamics of intramolecular electron transfer from ruthenium to copper. *Proc. Natl. Acad. Sci. USA.* 81:6554–6558.
30. Peterson-Kennedy, S. E., J. L. McGourty, and B. M. Hoffman. 1984. Temperature dependence of long-range electron transfer in [Zn,Fe$^{III}$] hybrid hemoglobin. *J. Am. Chem. Soc.* 106:5010–5012.
31. Marcus, R. A., and N. Sutin. 1975. Electron-transfer reactions with unusual activation parameters. A treatment of reactions accompanied by large entropy decreases. *Inorg. Chem.* 14:213–216.
32. Lauger, P., and G. Stark. 1970. Kinetics of carrier-mediated ion transport across lipid bilayer membranes. *Biochim. Biophys. Acta.* 211:458–466.
33. Hansen, U.-P., D. Gradmann, D. Sanders, and C. L. Slayman. 1981. Interpretation of current-voltage relationships for "active" ion transport systems: I. Steady-state reaction-kinetic analysis of class-I mechanisms. *J. Membr. Biol.* 63:165–190.
34. Pietrobon, D., and S. R. Caplan. 1985. Flow-force relationships for a six-state proton pump model: intrinsic uncoupling, kinetic equivalence of input and output forces, and domain of approximate linearity. *Biochemistry.* 24:5764–5776.
35. Miller, J. R., and J. Beitz. 1981. Long range transfer of positive

charge between dopant molecules in a rigid glassy matrix. *J. Chem. Phys.* 74:6746–6756.

36. Guarr, T., and G. McClendon. 1986. Quantum mechanical effects in inorganic and bioinorganic electron transfer. *Coord. Chem. Revs.* 68:1–52.

37. Siders, P., R. J. Cave, and R. A. Marcus. 1984. A model for orientation effects in electron-transfer reactions. *J. Chem. Phys.* 81:5613–5624.

38. Beratan, D. N., J. N. Onuchic, and J. J. Hopfield. 1985. Limiting forms of the tunneling matrix element in the long distance bridge mediated electron transfer problem. *J. Chem. Phys.* 83:5325–5329.

39. Laüger, P. 1979. A channel mechanism for electrogenic ion pumps. *Biochim. Biophys. Acta.* 552:143–161.

40. Thelen, M., P. S. O'Shea, and A. Azzi. 1985. New insights on the cytochrome c oxidase proton pump. *Biochem. J.* 227:163–167.

41. Brunori, M., P. Sarti, A. Colosimo, G. Antonini, F. Malatesta, M. G. Jones, and M. T. Wilson. 1985. Mechanism of control of cytochrome oxidase activity by the electrochemical-potential gradient. *EMBO J.* 4:2365–2368.

42. Rottenberg, H. 1979. Non-equilibrium thermodynamics of energy conversion in bioenergetics. *Biochim. Biophys. Acta.* 529:225–253.

43. Stucki, J. W. 1980. The optimal efficiency and the economic degrees of coupling of oxidative phosphorylation. *Eur. J. Biochem.* 109:269–283.

44. Caplan, S. R., and A. Essig. 1983. Bioenergetics and Linear Non-equilibrium Thermodynamics. Harvard University Press, Cambridge, MA. 435 pp.

45. Pietrobon, D., M. Zoratti, G. F. Azzone, J. W. Stucki, and D. Walz. 1982. Non-equilibrium thermodynamic assessment of redox-driven $H^+$ pumps in mitochondria. *Eur. J. Biochem.* 127:483–494.

46. Walz, D. 1983. Thermodynamics assessment of processes in isolated energy converting organelles. In Biological Structures and Coupled Flows. A. Oplatka and M. Balaban, editors. Academic Press, Inc., New York. 45–60.

47. Hill, T. L. 1983. Some general principles in free energy transduction. *Proc. Natl. Acad. Sci. USA.* 80:2922–2925.

48. Mitchell, P., and J. Moyle. 1969. Estimation of membrane potential and pH difference across the cristae membrane of rat liver mitochondria. *Eur. J. Biochem.* 7:471–484.

49. Nicholls, D. G. 1974. The influence of respiration and ATP hydrolysis on the proton-electrochemical gradient across the inner membrane of rat-liver mitochondria as determined by ion distribution. *Eur. J. Biochem.* 50:305–315.

50. Sorgato, M. C., S. J. Ferguson, D. B. Kell, and P. John. 1978. The protonmotive force in bovine heart submitochondrial particles. *Biochem. J.* 174:237–256.

51. Kell, D. B., P. John, and S. J. Ferguson. 1978. The protonmotive force in phosphorylating membrane vesicles from *Paracoccus denitrificans*. *Biochem. J.* 174:257–266.

52. Azzone, F. G., T. Pozzan, S. Massari, and M. Bragadin. 1978. Proton electrochemical gradient and rate of controlled respiration in mitochondria. *Biochim. Biophys. Acta.* 501:296–306.

53. Azzone, G. F., T. Pozzan, and S. Massari. 1978. Proton electrochemical gradient and phosphate potential in mitochondria. *Biochim. Biophys. Acta.* 501:307–316.

54. Brudvig, G. W., D. F. Blair, and S. I. Chan. 1984. Electron spin relaxation of $Cu_A$ and cytochrome a in cytochrome c oxidase. Comparison to heme, copper, and sulfur radical complexes. *J. Biol. Chem.* 259:11001–11009.

55. Vik, S. B., and R. A. Capaldi. 1980. Conditions for optimal electron transfer activity of cytochrome c oxidase isolated from beef heart mitochondria. *Biochem. Biophys. Res. Commun.* 94:348–354.

56a.Scheiner, S. 1981. Quantum chemical studies of proton transport in biomembranes. *Ann. N.Y. Acad. Sci.* 367:493–509.

56b.de la Vega, J. R. 1982. Role of symmetry in the tunnelling of the proton in double minimum potentials. *Accts. Chem. Res.* 15:185–191.

57. Knapp, E.-W., K. Schulten, and Z. Schulten. 1980. Proton conduction in linear hydrogen-bonded systems. *Chem. Phys.* 46:215–229.

58. Glasser, L. 1975. Proton conduction and injection in solids. *Chem. Rev.* 75:21–65.

59. Caplan, S. R. 1971. Nonequilibrium thermodynamics and its application to bioenergetics. *Curr. Top. Bioenerg.* 4:1–79.

60. Hansford, R. G. 1980. Control of mitochondrial substrate oxidation. *Curr. Top. Bioenerg.* 10:217–278.

61. Hunter, D. R., and R. A. Capaldi. 1974. Respiratory control in cytochrome oxidase. *Biochem. Biophys. Res. Commun.* 56:623–628.

62. Chance, B., and G. R. Williams. 1956. The respiratory chain and oxidative phosphorylation. *Adv. Enzymol.* 17:65–134.

63. Nicholls, D. G. 1979. Brown adipose tissue mitochondria. *Biochim. Biophys. Acta.* 549:1–29.

64. Mitchell, P. 1969. Chemiosmotic coupling and energy transduction. *Theor. Exp. Biophys.* 2:159–216.

65. Mitchell, P. 1985. Molecular mechanisms of protonmotive $F_0F_1$ ATPases. *FEBS (Fed. Eur. Biochem. Soc.) Lett.* 182:1–7.

66. Pietrobon, D., M. Zoratti, and G. F. Azzone. 1983. Molecular slipping in redox and ATPase $H^+$ pumps. *Biochim. Biophys. Acta.* 723:317–321.

67. Pietrobon, D., G. F. Azzone, and D. Walz. 1981. Effect of funiculosin and antimycin A on the redox-driven $H^+$-pumps in mitochondria: on the nature of "leaks." *Eur. J. Biochem.* 117:389–394.

68. Wilson, D. F., M. Erecinska, C. S. Owen, and L. Mela. 1974. Thermodynamic relationships in mitochondrial oxidative phosphorylation and respiratory control. In Dynamics of Energy-Transducing Membranes. L. Ernster, R. W. Estabrook, and E. C. Slater, editors. Elsevier (Amsterdam) 221–231.

69. Slater, E. C., J. Rosing, and A. Mol. 1973. The phosphorylation potential generated by respiring mitochondria. *Biochim. Biophys. Acta.* 292:534–553.

70. Chance, B., and G. R. Williams. 1955. Respiratory enzymes in oxidative phosphorylation. I. Kinetics of oxygen utilization. *J. Biol. Chem.* 217:383–393.

71. Copenhaver, J. H., Jr., and H. A. Lardy. 1952. Oxidative phosphorylations: pathways and yield in mitochondrial preparations. *J. Biol. Chem.* 195:225–238.

72. Ernster, L., and K. Nordenbrand. 1974. Phosphorylation potential and phosphorylating efficiency of respiring mitochondria. In Dynamics of Energy-Transducing Membranes. L. Ernster, R. W. Estabrook, and E. C. Slater, editors. Elsevier (Amsterdam). 283–288.

73. Sorgato, M. C., and S. J. Ferguson. 1979. Variable proton conductance of submitochondrial particles. *Biochemistry.* 18:5737–5742.

74. Sorgato, M. C., D. Branca, and S. J. Ferguson. 1980. The rate of ATP synthesis can be independent of the magnitude of the protonmotive force. *Biochem. J.* 188:945–948.

75. Sorgato, C., D. Branca, and S. J. Ferguson. 1979. Factors affecting the proton conductance of submitochondrial particles. In Function and Molecular Aspects of Biomembrane Transport. E. Quagliariello, F. Palmieri, S. Papa, and M. Klingenberg, editors. Elsevier/North Holland (Amsterdam). 213–216.

76. Duszynski, J., and L. Wojtczak. 1985. The apparent nonlinearity of the relationship between the rate of respiration and the protonmotive force of mitochondria can be explained by heterogeneity of mitochondrial preparations. *FEBS (Fed. Eur. Biochem. Soc.) Lett.* 182:243–248.

77. van Gelder, B. F., J. L. M. L. vanRijn, G. J. A. Schilder, and J. Wilms. 1977. The effect of pH on the half-reduction potentials of cytochrome c oxidase. In Structure and Function of Energy-Transducing Membranes. K. van Dam and B. F. van Gelder, editors. Elsevier/North Holland (Amsterdam). 61–68.

78. Nakao, K., and G. Palmer. 1983. Further characterization of the potentiometric behavior of cytochrome oxidase. Cytochrome *a* stays low-spin during oxidation and reduction. *J. Biol. Chem.* 258:14908–14913.

79. Wikström, M. K. F. 1974. The principle of energy transduction in the cytochrome *c* oxidase region of the respiratory chain. *Ann. N.Y. Acad. Sci.* 227:146–158.

80. Artzatbanov, V. Y., A. A. Konstantinov, and V. P. Skulachev. 1978. Involvement of intramitochondrial protons in redox reactions of cytochrome *a. FEBS (Fed. Eur. Biochem. Soc.) Lett.* 87:180–185.

81. Wikström, M. K. F. 1977. Proton pump coupled to cytochrome *c* oxidase in mitochondria. *Nature (Lond.).* 266:271–273.

82. Gelles, J., and S. I. Chan. 1985. Chemical modification of the $Cu_A$ center in cytochrome *c* oxidase by sodium p-hydroxymercuribenzoate. *Biochemistry.* 24:3963–3972.

83. Blair, D. F., S. N. Witt, and S. I. Chan. 1985. The mechanism of cytochrome *c* oxidase-catalyzed dioxygen reduction at low temperatures. Evidence for two intermediates at the three-electron level and entropic promotion of the bond-breaking step. *J. Am. Chem. Soc.* 107:7389–7399.

84. Babcock, G. T., P. M. Callahan, M. R. Ondrias, and I. Salmeen. 1981. Coordination geometries and vibrational properties of cytochromes *a* and $a_3$ in cytochrome oxidase from soret excitation raman spectroscopy. *Biochemistry.* 20:959–966.

85. Martin, C. T., C. P. Scholes, and S. I. Chan. 1985. The identification of histidine ligands to cytochrome *a* in cytochrome *c* oxidase. *J. Biol. Chem.* 260:2857–2861.

86. Diaddario, L. C., Jr., E. R. Dockal, M. D. Glick, L. A. Ochrymowycz, and D. B. Rorabachev. 1985. Structural changes accompanying electron transfer in copper(II)/copper(I) complexes involving related open-chain and cyclic tetrathia ether ligands. *Inorg. Chem.* 24:356–363.

87. Makinen, M. W., S. A. Schichman, S. C. Hill, and H. B. Gray. 1983. Heme-heme orientation and electron transfer kinetic behavior of multisite oxidation-reduction enzymes. *Science (Wash. DC).* 222:929–931.

88. Poulos, T. L., and J. Kraut. 1980. A hypothetical model of the cytochrome *c* peroxidase · cytochrome *c* electron transfer complex. *J. Biol. Chem.* 255:10322–10330.

89. Hill, T. L. 1977. Free Energy Transduction in Biology. Ch. 1–2. Academic Press, Inc., New York.